Patterns of reduced cortical thickness and striatum pathological morphology in cocaine addiction.

Eduardo A Garza-Villarreal[*,1,2], Ruth Alcalá-Lozano[1], Thania Balducci[1,3], Diego Ángeles-Valdéz4, M. Mallar Chakravarty[5,6,7], Gabriel A. Devenyi[5,6], Jorge J Gonzalez-Olvera[1].

[1] Subdirección de Investigaciones Clínicas, Instituto Nacional de Psiquiatría "Ramón de la Fuente Muñiz", Mexico City, Mexico
[2] Center of Functionally Integrative Neuroscience (CFIN) and MINDLab, Department of Clinical Medicine, Aarhus University, Aarhus, Denmark
[3]Graduate School of Medical Sciences, Universidad Nacional Autónoma de México, Mexico City, Mexico.
[4]Faculty of Psychology, Universidad Nacional Autónoma de México, Mexico City, Mexico.
[5]Cerebral Imaging Centre, Douglas Mental Health University Institute, Montreal, QC, Canada.
[6] Department of Psychiatry, McGill University, Montreal, Canada
[7] Department of Biomedical Engineering, McGill University, Montreal, Canada

Corresponding author:

Eduardo A. Garza-Villarreal, M.D., Ph.D.

Subdireccion de Investigaciones Clinicas,
Instituto Nacional de Psiquiatria "Ramón de la Fuente Muñiz",
Calzada Mexico-Xochimilco 101,
Col. San Lorenzo Huipulco, Delegación Tlalpan,
C.P. 14370, Mexico City, Mexico
Phone: +52 (55) 41605354
Email: egarza@imp.edu.mx

Abstract

Substance addiction is regarded as an important public health problem, perpetuated by fronto-striatal circuit pathology. A usual finding in neuroimaging human and murine studies is cortical thinning and lower volume when compared to healthy controls. In this study we wished to replicate cortical thinning findings and find if striatum morphology may explain the cortical pathology. For this we analyzed T1w neuroimaging data from an ongoing addiction Mexican dataset. This dataset includes cocaine addicts diagnosed by expert psychiatrists and healthy controls. For the analysis we used voxel-based morphometry, cortical thickness and volumetric analysis of the basal ganglia, and we correlated striatum volume with cortical thickness to find pathological patterns. Our group contrast showed cortical thinning and striatum volume differences in cocaine addicts correlated to their years of substance use, craving and age. Our correlation between striatum-cortex morphology showed higher significant correlations in healthy controls, not observed in cocaine addicts. The correlation between striatum volume and cortical thickness in healthy controls involved similar areas as those shown with less cortical thickness in cocaine addicts. We suggest that striatum morphological changes in addiction may explain the pattern of cortical thinning observed across several substances addiction studies.

Research Data Related to this Submission

Data set https://zenodo.org/record/1409808#.W5E3oCOZPIF

Patterns of reduced cortical thickness and striatum pathological morphology in cocaine addiction

This dataset includes all the data and scripts needed to reproduce the analysis and results on the manuscript "Patterns of reduced cortical thickness and striatum pathological morphology in cocaine addiction" (link). The brain data is not raw, as T1w were not defaced. We will do so in the near future for version 2.0. Instead we include only the "output/thickness" files used in the final analysis. For the use of raw T1w images, please contact the main author EAGV.

Introduction

Substance addiction is a generalized problem in the world accompanied by important psychiatric comorbidities and exacerbated by poor treatment outcomes [1]. In Mexico, cocaine is the second most used illegal substance of abuse among the population of users, and it inflicts social, family, economical and health problems (https://www.gob.mx/salud%7Cconadic/acciones-y-programas/encuesta-nacional-de-consumo-de-drogas-alcohol-y-tabaco-encodat-2016-2017-136758). Volkow et al. [2] have proposed a hypothesis that substance addiction is a pathological cycle of behavior, and that chronic drug use directly and indirectly affects brain areas such as the striatum and thalamus and their cortical connectivity. Such neurobiological changes perpetuate and potentially reinforce the addiction cycle. The consistent reinforcement of this cycle leads to addictive behaviors commonly observed in individuals suffering from addiction [3]. As a result, a brain circuit involving the striatum, thalamus and prefrontal areas is commonly studied to better understand how brain function and structure is altered in those suffering from addictions [4,5]. Recent studies in humans and murine models have supported pathological fronto-striatal connectivity as the main driver of the addiction cycle and substance seeking [6,7].

Human neuroimaging studies using voxel-based morphometry (VBM) and cortical thickness (CT) have typically demonstrated variable brain differences, usually including decreased volume or CT in prefrontal, temporal, occipital and subcortical areas in the brains of addicts [8-13], although there have been increase volume findings in striatum [14]. The decrease in these measures is usually correlated with behavioral (i.e. substance craving) and cognitive measures [15,16]. A meta-analysis in cocaine and methamphetamine addicts found lower volume on bilateral insula, left thalamus, left middle frontal gyrus (lmFG), right anterior cingulate (rACC) and right inferior frontal gyrus (rIFG) [17]. Parvaz et al [18] recently demonstrated that the volume of the inferior frontal gyrus (IFG) and the medial prefrontal cortex (mPFC) increase following treatment for cocaine addiction. These studies suggest brain morphology is highly affected in addiction, and that treatment success can partly revert this damage. These areas found with reduced volume or CT in addiction such as the insula, IFG, mPFC, ACC, have also been found connected structurally and functionally to the different nuclei of the striatum [19]. If striatum is a region highly affected in addiction and it is intimately connected with these cortical areas, which in turn seem to be commonly found affected in addiction, pathological morphological changes in striatum may help explain the reduction of cortical thickness and volume in such widespread areas of the cortex.

In this study, we wish to find neuroanatomical differences between cocaine addicts and matched healthy controls, to better understand the toxic effect of drug use and the effect of craving. We also wanted to study the relation between striatum structure and cortical thickness. For this, we used novel computational anatomy algorithms to perform volumetric analysis, cortical thickness extraction and subcortical segmentation of striatum and thalamus.

Materials and Methods

Participants

We recruited 160 participants as part of a principal multidisciplinary addiction study at the Instituto Nacional de Psiquiatría "Ramón de la Fuente Muñiz" in Mexico City, Mexico. Of those, 49 participants did not fulfill the inclusion criteria. We diagnosed cocaine dependence using the MINI International Neuropsychiatric Interview Spanish version [20], which was administered by trained psychiatrists. For inclusion, cocaine consumption had to be active or with abstinence less than 60 days prior to the scan, with frequency of use of at least three days per week and no more than 60 continued days of abstinence during the last 12 months. There could be polysubstance use, however cocaine had to be the drug of impact. Additional exclusion criteria for both groups were: somatic diseases, neurological disorders, severe suicidal risk, history of head trauma with loss of consciousness, pregnancy, obesity, severe psychiatric disorders and non-compliance with magnetic resonance imaging safety standards. A final sample of 64 cocaine addicts (AD) (7 female) and 47 healthy controls (HC) (8 female) were included in our study. Healthy controls were matched as closely as possible by age (± 2y), sex and handedness. Education was matched as closely as possible, though it has significantly higher in HC, therefore education was added as a covariate in the statistical analysis. Table 1 describe the demographic and addiction related information. The study was approved by the local ethics committee and performed at the Instituto Nacional de Psiquiatría "Ramón de la Fuente Muñiz" in Mexico City, Mexico. The study was carried out according to the Declaration of Helsinki. All participants were invited through posters placed in several centers for addiction treatment and through the Institute's addiction clinic for outpatients. Healthy controls were recruited from the Institute (i.e. administrative workers, their family, etc) and using Internet social outlets. Participants provided verbal and written informed consent. The participants underwent clinical and cognitive tests besides the MRI as part of the main ongoing addiction database. Participants were asked to abstain from drug use for at least 24 hours prior to the study and were urine-tested for the presence of the drugs and a breath determination of alcohol in the blood before the MRI scan. The clinical, cognitive and MRI sessions were performed either the same day as minimum, or 4 days apart as maximum. It is important to point out none of our participants were homeless or in extreme poverty.

Table 1. Demographic and substance addiction variables between groups.

Variable	**HC**	**AD**	**p**
	(N=47)	(N=64)	
Age	30.7 ±7.6	31.0 ±7.2	0.846
Sex			0.519
- F	8 (17.0%)	7 (10.9%)	
- M	39 (83.0%)	57 (89.1%)	

Education	3.7 ±1.5	2.9 ±1.2	0.003
Handedness			0.99
- A	3 (6.4%)	4 (6.2%)	
- L	4 (8.5%)	5 (7.8%)	
- R	40 (85.1%)	55 (85.9%)	
BIS Total	40.6 ±11.5	60.9 ±15.2	< .001
• BIS ICog	11.9 ±3.7	17.2 ± 5.4	< .001
• BIS IMo	12.7 ±6.0	18.2 ±7.5	< .001
• BIS INoPl	15.9 ±5.6	25.5 ±7.6	< .001
Cigarettes per day (tobacco)	1.2 ±1.4	3.7 ±4.4	0.006
Initial Age	-	21.67 ±6.15	-
Years of Consumption	-	9.3 ±6.58	-
Craving (CCQ General)	-	140 ±42.49	-

HC = Healthy Control; AD = Cocaine Addict; F = female; M = male; A = Ambidexterous; L = Left handed, R = Right handed, BIS = Barrat Impulsivity Scale; ICog = Cognitive; IMo = Motor; INoPl = Non-Planning; CCQ = Cocaine Craving Quotient.

Clinical measures

Craving in the last month and at the interview was measured using the cocaine craving questionnaire (CCQ) [21]. Self-reported impulsivity was evaluated with the Barratt Impulsiveness Scale (BIS-11), which has three subscales: non-planning impulsiveness, which involves a lack of forethought; cognitive impulsivity, which involves making quick decisions; and motor impulsivity, which involves acting without thinking [22].

MRI Acquisition

T1-weighted brain data were acquired using a Philips Ingenia 3T Magnetic Resonance Imaging (MRI) system (Philips Healthcare, Best, Netherlands & Boston, MA, USA) with a 32-channel dS Head coil. T1-weighted images were acquired using a 3D FFE SENSE sequence, TR/TE = 7/3.5 ms, FOV = 240, matrix = 240 x 240 mm, 180 slices, gap = 0, plane = Sagittal, voxel = 1 x 1 x 1 mm (5 participants were acquired with a voxel size = .75 x .75 x 1 mm), scan time = 3.19 min. As part of the principal addiction database, resting state fMRI, High Angular Resolution Diffusion Imaging (HARD), and Diffusion Kurtosis Imaging (DKI) sequences were also acquired and are not part of this study. The order of the sequences was: rsfMRI, T1w, HARDI, DKI, and was maintained across participants. Total scan time was ~50 minutes.

Image preprocessing and processing

T1-weighted images were converted from DICOM format to MINC for preprocessing. T1 images were preprocessed using an in-house preprocessing pipeline with the software Bpipe (https://github.com/CobraLab/minc-bpipe-library)[23], which makes use of the MINC Tool-Kit (http://www.bic.mni.mcgill.ca/ServicesSoftware/ServicesSoftwareMincToolKit) and ANTs [24]. Briefly, we performed N4 bias field correction [25], linear registration to MNI-space using ANTs, we cropped the region around the neck in order improve registration quality, followed by transformation back to native space, and created whole-brain masks.

We estimated volume-based (VBM) and surfaced-based variables (cortical thickness [CT] and surface area [SA]) using the CIVET processing pipeline (version 1.1.12; Montreal Neurological Institute). First, the T1w images were linearly aligned to the ICBM 152 average template using a 9-parameter transformation (3 translations, rotations, and scales) [26] and preprocessed to minimize the effects of intensity non-uniformity [27]. The images were then classified into three main tissues: gray matter (GM), white matter (WM) and cerebrospinal fluid (CSF) [28]. GM was used for VBM. The hemispheres were modeled as GM and WM surfaces using a deformable model strategy that generates 4 separate surfaces defined by 40962 vertices each [29]. CT was derived between homologous vertices on GM and WM derived using the t-link metric and blurred with a 20 mm surface-based diffusion kernel, while SA was estimated by averaging across the adjoining faces at each vertex [30]. Native-space thicknesses were used in all analyses reported [31,32]. Homology across the population was achieved using a non-linear surface-based normalization that utilizes a mid-surface (between pial and WM surfaces) [33]. This normalization uses a depth-potential function [34] that fits each subject to a minimally biased surface-based template [35].

For the subcortical analysis, the native space preprocessed files were input into the MAGeT-Brain morphological analysis pipeline (http://cobralab.ca/software/MAGeTbrain.html) [36]. MAGeT-Brain is modified multi-atlas segmentation technique designed to take advantage of hard-to-define atlases and uses a minimal number of atlases for input into the segmentation process. The used a basal ganglia atlas [37] obtained by manual segmentation of one brain. We obtained segmentation and volume measures for striatum, thalamus and globus pallidus.

Statistical analysis

Voxel based morphometry (VBM) gray matter and vertex-wise analyses were performed with the RMINC package (https://wiki.phenogenomics.ca/display/MICePub/RMINC) in R statistics and RStudio [38]. Public packages used for the analysis were: tidyverse, psych, pastecs, moonBook and plotrix. The general linear model included “CT” as the dependent variable, “group” as the between subjects variable, and “age”, “sex” and “education” as covariates. All analyses were corrected for multiple comparisons using the false discovery rate (FDR) at 10% [39]. From the resulting significant peaks we extracted MNI coordinates and labels based on the AAL

atlas [40], except for VBM in which we used Harvard-Oxford Cortical Atlas [41-44]. As post-hoc, we calculated the correlation coefficient between years of consumption and craving, and all the significant peaks CT. Using that matrix, we statistically analyzed only correlations that exceeded a chosen threshold of r = ± 0.2 (low-medium effect size) using the t-distribution with an alpha of 0.05. We then used the FDR to adjust the p-value for multiple comparisons of the correlations. As a side note, VBM was only calculated because it is a more widely used measure of brain morphology. Because we were more interested in cortical thickness, we did not further analyze this measure. However, tools such as BrainMap (http://brainmap.org) would be able to use this data for future meta-analyses.

Basal ganglia analysis

We studied basal ganglia volumes using a general linear model that included subcortical volume as the dependent variable, group as the between-subjects variable, and age, sex and education as covariates. Our previous study in cocaine addiction showed mainly group x age interactions in striatum volume [45], hence we performed that interaction model as well. We then calculated the correlation coefficient between years of consumption and craving, and all basal ganglia including their striatum and thalamus segmentation. Using that matrix, we statistically analyzed only correlations that exceeded a chosen threshold of r = ± 0.2 (low-medium effect size) using the t-distribution with an alpha of 0.05. Because basal ganglia volume is relative to whole-brain volume, we then performed partial correlations controlling for whole-brain volume.

Striatum-cortex correlation analysis

The covariation between striatum subnuclei that were correlated significantly with years of consumption and craving (left nucleus accumbens and right precommissural precuneus), and whole-brain cortical thickness was studied using a similar approach to the “Mapping anatomical correlations across cerebral cortex (MACACC)” analysis method [46]. The MACACC method is performed by selecting a seed region of interest (ROI) and correlating the CT of this ROI with the CT of all brain vertices. This approach is similar to functional connectivity analysis [47,48]. The resulting statistic gives an indication of the degree to which CT throughout the brain covaries with the ROI across subjects and can be used to estimated the structural and functional connectivity between different areas. As our ROI, we chose to instead use the volume of the significant nuclei in the partial correlation analysis: left nucleus accumbens and right pre-commissural putamen volume (basal ganglia analysis). We also chose whole left and right striatum volume to corroborate our results. This method has been used successfully [49]. We then correlated the volume of each ROI against the brain vertices for all participants, and then each group separately. All maps were FDR corrected at 5% due to the high distribution of significant peaks.

Results

We found significantly lower volume (Supplementary Figure 1 & Table 1) and cortical thickness in cocaine addicts in mainly prefrontal areas (Figure 1 and Supplementary Table 2). VBM showed 2 small clusters of increased volume that were not found in the CT analysis. Surface area was not significant.

Insert Figure 1

The post-hoc analysis showed that years of cocaine consumption and craving were significantly correlated with several CT peaks (Supplementary Figs. 2 and 3, Supplementary Tables 2 and 3). The subcortical analysis showed a significant lower volume in left thalamus of the AD group ($F(1,104) = 4.723$, $p = 0.03$) (Supplementary Fig. 4) than the HC group. There was no difference in striatum and globus pallidus volume. There was, however, a significant group x age interaction in left and right striatum volume (Figure 2) at alpha 0.1 (left: $F(1,103) = 2.83$, $p = 0.1$; right: $F(1,103) = 3.26$, $p = 0.07$), which was similar to our previous findings [45].

Insert Figure 2

The bivariate correlation analysis of years of consumption and craving with basal ganglia volumes, showed no significant results. The partial correlation analysis controlling for whole-brain volume showed significant negative correlation between: 1) years of consumption and left nucleus accumbens ($r = -0.23$, $t = -2.46$, $p = 0.02$), and 2) craving and right pre-commissural putamen ($r = -0.27$, $t = -2.89$, $p = 0.005$).

The striatum-cortex correlation analysis results using the ROIs: 1) left nucleus accumbens (lNAcc) and 2) right pre-commisual putamen (rPrePut), are shown in Figure 3. The result of left and right whole striatum volume are in the Supplementary Figure 5. The resulting significant covariance maps show lNAcc and rPrePut volumes are related to similar areas that showed lower cortical thickness in AD in the CT group comparison (Figure 1). A subset analysis showed that the correlation between lNAcc and cortex in AD is nonexistent compared to HC. The subset analysis of correlation between rPrePut and cortex showed higher significant correlations in HC than the AD group. For this last analysis, significant brain areas of correlation shared between groups are shown in Table 2. As for whole striatum volume, we also found higher correlation in HC compared to AD. All peak tables are shown in Supplementary Tables 5 to 15. In general, striatum volume in AD showed low correlation to cortical thickness compared to healthy controls.

Insert Figure 3

Table 2. Significant peaks in similar brain areas between groups in the correlation analysis between right precommissural putamen and cortical thickness.

	HC					AD				
Brain Area	**vertex**	**x**	**y**	**z**	**t**	**vertex**	**x**	**y**	**z**	**t**
Left Superior temporal gyrus	10435	-41	-18	-1	3.28	13033	-44	3	-15	4.86
Left Middle temporal gyrus	35910	-61	-54	-7	3.75	13282	-49	13	-29	4.36
Left Inferior occipital gyrus	576	-59	-60	-9	3.92	33470	-36	-88	-17	4.18
Left Precentral gyrus	26769	-24	-3	54	2.88	20887	-53	-5	30	3.94

HC = healthy controls, AD = cocaine addicts, vertex = Surface vertex CIVET 1.1.12, t = tvalue.

Discussion

In our study, Mexican cocaine addicts showed lower gray matter volume and cortical thickness in several brain areas, with the most extensive difference on prefrontal cortex. Cortical thickness and striatal subnuclei volume were significantly correlated to years of cocaine use and craving. The covariation between striatal whole and subnuclei volumes, and cortical thickness suggests close neuroanatomical pathology of fronto-striatal areas in cocaine addicts.

Using VBM and CT analysis we found significantly lower values in cocaine addicts (AD) than healthy controls (HC). In VBM we found increased volume in two areas that were not found in the CT analysis, probably due to the differences between methods. These findings of cortical thinning are not surprising as they have been shown in other studies of different type of addiction [9,10,50], corroborating cortical pathology from chronic cocaine use. The cortical thinning was observed in areas of all cortical lobes, slightly lateralized to the left hemisphere. Although we did not find group differences between volumes in striatum, we found an age x group interaction that suggests a pathological development related to addiction and or chronic use. The striatal subnuclei nucleus accumbens and precommissural putamen were correlated with years of cocaine use and craving. Striatum volume differences, when compared to healthy controls, can be present or absent, higher or lower, in different studies [14,51], which suggests either a complex pathology when measured with these methods or differences in volumetric and segmentation methods. Nevertheless, animal and humans studies corroborate the involvement of the striatum in addiction and affectation of its morphology [52-54].

A landmark study by Chen et al [6] using optogenetics showed that seeking for cocaine in addicted mice could be effectively stopped by stimulating the prelimbic cortex (mPFC or DLPFC in human), while inhibiting this region induced the opposite effect, increased cocaine seeking. In humans, a similar effect has been observed by stimulating the DLPFC using rTMS where cocaine addicts report reduced craving and cocaine use [55]. The fronto-striatal circuit is involved in response inhibition, which is found to be greatly affected in cocaine

addiction in animal models and in human studies, and this circuit includes the striatum, thalamus, globus pallidus, primary motor cortex, ACC, dmPFC and the vlPFC [5]. However, the structural connectivity between the striatum and cerebral cortex seems to be more extended, involving also areas such as the SFG, IFG, temporal pole and occipital cortex [19]. Substance addiction is a complex condition and at the moment the main hypothesis for the etiology of the addictive cycle is the fronto-striatal circuit pathology [2,56]. Although the causal direction of the pathology (fronto-striatal or striato-frontal) has not been demonstrated yet, the involvement of dopamine receptors in striatum suggests a mainly striatal pathology [57].

The covariation between lNAcc/rPrePut volume and CT of all participants (striatum-cortex covariation) seems to follow a similar pattern to the structural connectivity of the striatum. Interestingly, not only our group contrast map of lower CT in cocaine addicts shows similarities with the striatum-cortex covariation, but also this covariation was only observed in healthy controls and it almost disappeared in cocaine addicts. This could be an indication of the underlying pathological changes in striatum or cortex (or both), secondary to cocaine addiction or chronic use. This shared morphological finding have been shown in young adult smokers with lower CT in frontal cortical areas and higher volume of the caudate [58]. In a study with several types of substances, another study showed lower volume in frontal areas as well as the caudate nucleus, among others [59]. As for the involvement of striatum pathology and cortex morphology in human addiction, a recent study showed that striatal D1-type receptor (dopamine) levels are correlated with mean global cortical thickness in methamphetamine users but not in controls, specifically in temporal and occipital lobes [60]. The authors suggest this abnormality may be a cortical adaptation to chronic substance use with involvement of the D1-type. The evidence highly suggests that the observed morphological findings in cortex may be due to either striatum pathology, or cortical pathology may drive the striatum changes that engrain this pathology. Confirming a causal relationship would help explain the shared cortical findings across types of substance addiction and would corroborate the hypothesis about dopamine related fronto-striatal dysfunction as one of the main causes of human substance addiction.

Our study has several limitations. Correlational studies cannot prove causality as they can only suggest relationships that can be studied further in real experimental designs. However, it is obvious that experimental designs in substance addiction are unethical in humans; hence we rely on animal studies and correlational designs in humans to provide knowledge. Our significant threshold for the multiple comparisons FDR in the CT analysis was 10% ($q = 0.1$), which may be considered more liberal than usual and caution should be taken when interpreting our findings. However, this approach was preferred to allow for a more exploratory study and we have successfully used it in our previous studies. Our dataset is unique and ongoing, and because addiction and polysubstance use is complex, we wanted to avoid false negatives. The corroboration of our results in relation to other studies seem to support our use of a more relaxed threshold in this particular sample. Our sample is mainly males due to the prevalence of cocaine addiction in this sex, which is a problem in all cocaine addiction studies.

Our results show a possible relation between striatum volume and cortical thinning in cocaine addiction, which further confirms fronto-striatal pathology. Specifically, we believe our results suggest that the pattern of cortical thinning found in most addiction studies may be explained by striatal pathology. Future studies should aim at corroborating the cortical connectivity between striatum and cortex in substance addiction using advance non-invasive diffusion methods.

Acknowledgements

We would like to thank Rocio Estrada Ordoñez and Isabel Lizarindari Espinosa Luna at the Unidad de Atención Toxicologica Xochimilco for all their help and effort. Finally, we thank the study participants for their cooperation and patience. This project was funded by CONACYT-FOSISS-S0008 project No. 0260971, No. 0201493 and CONACYT-Cátedras project No. 2358948. For the use of the Harvard-Oxford Atlas, we are very grateful for the training data for FIRST, particularly to David Kennedy at the CMA, and also to: Christian Haselgrove, Centre for Morphometric Analysis, Harvard; Bruce Fischl, Martinos Center for Biomedical Imaging, MGH; Janis Breeze and Jean Frazier, Child and Adolescent Neuropsychiatric Research Program, Cambridge Health Alliance; Larry Seidman and Jill Goldstein, Department of Psychiatry of Harvard Medical School; Barry Kosofsky, Weill Cornell Medical Center.

Conflicts of Interest

The authors declare no conflicts of interest.

References

1 Alvarez Y, Pérez-Mañá C, Torrens M, Farré M. Antipsychotic drugs in cocaine dependence: a systematic review and meta-analysis. *J Subst Abuse Treat* 2013; **45**: 1–10.

2 Volkow ND, Koob GF, McLellan AT. Neurobiologic Advances from the Brain Disease Model of Addiction. *N Engl J Med* 2016; **374**: 363–371.

3 Volkow ND, Morales M. The Brain on Drugs: From Reward to Addiction. *Cell* 2015; **162**: 712–725.

4 Goldstein RZ, Volkow ND. Drug addiction and its underlying neurobiological basis: neuroimaging evidence for the involvement of the frontal cortex. *Am J Psychiatry* 2002; **159**: 1642–1652.

5 Morein-Zamir S, Robbins TW. Fronto-striatal circuits in response-inhibition: Relevance to addiction. *Brain Res* 2015; **1628**: 117–129.

6 Cheng X, Li T, Zhou H, Zhang Q, Tan J, Gao W *et al.* Cortical electrical stimulation with varied low frequencies promotes functional recovery and brain remodeling in a rat model of ischemia. *Brain Res Bull* 2012; **89**: 124–132.

7 Smith WC, Rosenberg MH, Claar LD, Chang V, Shah SN, Walwyn WM *et al.* Frontostriatal Circuit Dynamics Correlate with Cocaine Cue-Evoked Behavioral Arousal during Early Abstinence. *eNeuro* 2016; **3**. doi:10.1523/ENEURO.0105-16.2016.

8 Makris N, Gasic GP, Kennedy DN, Hodge SM, Kaiser JR, Lee MJ *et al.* Cortical Thickness Abnormalities in Cocaine Addiction—A Reflection of Both Drug Use and a Pre-existing Disposition to Drug Abuse? *Neuron* 2008; **60**: 174–188.

9 Kühn S, Schubert F, Gallinat J. Reduced thickness of medial orbitofrontal cortex in smokers. *Biological Psychiatry* 2010; **68**: 1061–1065.

10 Durazzo TC, Tosun D, Buckley S, Gazdzinski S, Mon A, Fryer SL *et al.* Cortical Thickness, Surface Area, and Volume of the Brain Reward System in Alcohol Dependence: Relationships to Relapse and Extended Abstinence. *Alcoholism: Clinical and Experimental Research* 2011; **35**: 1187–1200.

11 Lopez-Larson MP, Bogorodzki P, Rogowska J, McGlade E, King JB, Terry J *et al.* Behavioural Brain Research. *Behavioural Brain Research* 2011; **220**: 164–172.

12 Ersche KD, Barnes A, Jones PS, Morein-Zamir S, Robbins TW, Bullmore ET. Abnormal structure of frontostriatal brain systems is associated with aspects of impulsivity and compulsivity in cocaine dependence. *Brain* 2011; **134**: 2013–2024.

13 Pehlivanova M, Wolf DH, Sotiras A, Kaczkurkin A, Moore TM, Ciric R *et al.* Diminished Cortical Thickness is Associated with Impulsive Choice in Adolescence. *Journal of Neuroscience* 2018; : 2200–17.

14 Ersche KD, Jones PS, Williams GB, Turton AJ, Robbins TW, Bullmore ET. Abnormal brain structure implicated in stimulant drug addiction. *Science* 2012; **335**: 601–604.

15 Ersche KD. Neurobiological correlates of the familial risk for stimulant drug dependence. *Neuropsychopharmacology* 2013; **38**: 238–239.

16 Levar N, Francis AN, Smith MJ, Ho WC, Gilman JM. Verbal Memory Performance and Reduced Cortical Thickness of Brain Regions Along the Uncinate Fasciculus in Young Adult Cannabis Users. *Cannabis and Cannabinoid Research* 2018; **3**: 56–65.

17 Ersche KD, Williams GB, Robbins TW, Bullmore ET. Meta-analysis of structural brain abnormalities associated with stimulant drug dependence and neuroimaging of addiction vulnerability and resilience. *Current Opinion in Neurobiology* 2013; **23**: 615–624.

18 Parvaz MA, Moeller SJ, d'Oleire Uquillas F, Pflumm A, Maloney T, Alia-Klein N *et al.* Prefrontal gray matter volume recovery in treatment-seeking cocaine-addicted individuals: a longitudinal study. *Addict Biol* 2017; **22**: 1391–1401.

19 Jarbo K, Verstynen TD. Converging structural and functional connectivity of orbitofrontal, dorsolateral prefrontal, and posterior parietal cortex in the human striatum. *Journal of Neuroscience* 2015; **35**: 3865–3878.

20 Ferrando L, Soto M, Bobes J, Soto O, Franco L, Gibert J. Mini International Neuropsychiatric Interview (Spanish version 5.0). *Madrid: Institute IAP* 2000.

21 Sussner BD, Smelson DA, Rodrigues S, Kline A, Losonczy M, Ziedonis D. The validity and reliability of a brief measure of cocaine craving. *Drug Alcohol Depend* 2006; **83**: 233–237.

22 Oquendo MA, Baca-García E, Graver R, Morales M, Montalvan V, Mann J. Spanish adaptation of the Barratt impulsiveness scale (BIS-11). *European Journal of Psychiatry* 2001; **15**: 147–155.

23 Sadedin SP, Pope B, Oshlack A. Bpipe: a tool for running and managing bioinformatics pipelines. *Bioinformatics* 2012; **28**: 1525–1526.

24 Avants BB, Tustison N, Song G. *Advanced Normalization Tools (ANTS) Release 1.5*. University of Pennsylvania, 2011.

25 Tustison NJ, Avants BB, Cook PA, Zheng Y, Egan A, Yushkevich PA *et al.* N4ITK: improved N3 bias correction. *IEEE Trans Med Imaging* 2010; **29**: 1310–1320.

26 Collins DL, Collins DL, Neelin P, Neelin P, Peters TM, Peters TM *et al.* Automatic 3D intersubject registration of MR volumetric data in standardized Talairach space. *J Comput Assist Tomogr* 1994; **18**: 192–205.

27 Sled JG, Zijdenbos AP, Evans AC. A nonparametric method for automatic correction of intensity nonuniformity in MRI data. *IEEE Trans Med Imaging* 1998; **17**: 87–97.

28 Zijdenbos AP, Forghani R, Evans AC. Automatic 'pipeline' analysis of 3-D MRI data for clinical trials: application to multiple sclerosis. *IEEE Trans Med Imaging* 2002; **21**: 1280–1291.

29 Kim JS, Singh V, Lee JK, Lerch J, Ad-Dab'bagh Y, MacDonald D *et al.* Automated 3-D extraction and evaluation of the inner and outer cortical surfaces using a Laplacian map and partial volume effect classification.

Human Brain Mapping Journal 2005; **27**: 210–221.

30 Lerch JP, Evans AC. Cortical thickness analysis examined through power analysis and a population simulation. *NeuroImage* 2005; **24**: 163–173.

31 YYasser A-D, Singh V, Robbins S, Lerch J, Lyttelton O, Fombonne E *et al.* Native-space cortical thickness measurement and the absence of correlation to cerebral volume. *11th Annual Organization for Human Brain Mapping Meeting* 2005; : 1–1.

32 Sowell ER, Sowell ER, Peterson BS, Peterson BS, Kan E, Kan E *et al.* Sex Differences in Cortical Thickness Mapped in 176 Healthy Individuals between 7 and 87 Years of Age. *Cerebral Cortex* 2007; **17**: 1550–1560.

33 Robbins S, Evans AC, Collins DL, Whitesides S. Tuning and comparing spatial normalization methods. *Med Image Anal* 2004; **8**: 311–323.

34 Boucher M, Whitesides S, Evans A. Depth potential function for folding pattern representation, registration and analysis. *Med Image Anal* 2009; **13**: 203–214.

35 Lyttelton O, Boucher M, Robbins S, Evans A. An unbiased iterative group registration template for cortical surface analysis. *Human Brain Mapping Journal* 2007; **34**: 1535–1544.

36 Chakravarty MM, Steadman P, van Eede MC, Calcott RD, Gu V, Shaw P *et al.* Performing label-fusion-based segmentation using multiple automatically generated templates. *Hum Brain Mapp* 2013; **34**: 2635–2654.

37 Chakravarty MM, Bertrand G, Hodge CP, Sadikot AF, Collins DL. The creation of a brain atlas for image guided neurosurgery using serial histological data. *Human Brain Mapping Journal* 2006; **30**: 359–376.

38 Team R. *RStudio: Integrated Development for R. RStudio, Inc., Boston, MA URL http://www.rstudio.com/*. 2015.

39 Genovese CR, Lazar NA, Nichols T. Thresholding of statistical maps in functional neuroimaging using the false discovery rate. *Human Brain Mapping Journal* 2002; **15**: 870–878.

40 Schmahmann JD, Doyon J, McDonald D, Holmes C, Lavoie K, Hurwitz AS *et al.* Three-dimensional MRI atlas of the human cerebellum in proportional stereotaxic space. *Human Brain Mapping Journal* 1999; **10**: 233–260.

41 Frazier JA, Chiu S, Breeze JL, Makris N, Lange N, Kennedy DN *et al.* Structural brain magnetic resonance imaging of limbic and thalamic volumes in pediatric bipolar disorder. *Am J Psychiatry* 2005; **162**: 1256–1265.

42 Makris N, Goldstein JM, Kennedy D, Hodge SM, Caviness VS, Faraone SV *et al.* Decreased volume of left and total anterior insular lobule in schizophrenia. *Schizophrenia Research* 2006; **83**: 155–171.

43 Desikan RS, Ségonne F, Fischl B, Quinn BT, Dickerson BC, Blacker D *et al.* An automated labeling system for subdividing the human cerebral cortex on MRI scans into gyral based regions of interest. *NeuroImage* 2006; **31**: 968–980.

44 Goldstein JM, Seidman LJ, Makris N, Ahern T, O'Brien LM, Caviness VS *et al.* Hypothalamic abnormalities in schizophrenia: sex effects and genetic vulnerability. *Biological Psychiatry* 2007; **61**: 935–945.

45 Garza-Villarreal EA, Chakravarty MM, Hansen B, Eskildsen SF, Devenyi GA, Castillo-Padilla D *et al.* The effect of crack cocaine addiction and age on the microstructure and morphology of the human striatum and thalamus using shape analysis and fast diffusion kurtosis imaging. *Transl Psychiatry* 2017; **7**: e1122.

46 Lerch JP, Worsley K, Shaw WP, Greenstein DK, Lenroot RK, Giedd J *et al.* Mapping anatomical correlations across cerebral cortex (MACACC) using cortical thickness from MRI. *NeuroImage* 2006; **31**: 993–1003.

47 Friston KJ. Testing for anatomically specified regional effects. *Hum Brain Mapp* 1997; **5**: 133–136.

48 Worsley KJ, Chen J-I, Lerch J, Evans AC. Comparing functional connectivity via thresholding correlations and singular value decomposition. *Philos Trans R Soc Lond, B, Biol Sci* 2005; **360**: 913–920.

49 Ameis SH, Ducharme S, Albaugh MD, Hudziak JJ, Botteron KN, Lepage C *et al.* Cortical Thickness, Cortico-Amygdalar Networks, and Externalizing Behaviors in Healthy Children. *Biological Psychiatry* 2014; **75**: 65–72.

50 Kaag AM, Crunelle CL, van Wingen G, Homberg J, van den Brink W, Reneman L. Relationship between trait impulsivity and cortical volume, thickness and surface area in male cocaine users and non-drug using controls. *Drug Alcohol Depend* 2014; **144**: 210–217.

51 Barrós-Loscertales A, Garavan H, Bustamante JC, Ventura-Campos N, Llopis JJ, Belloch V *et al.* Reduced striatal volume in cocaine-dependent patients. *Human Brain Mapping Journal* 2011; **56**: 1021–1026.

52 Wheeler AL, Lerch JP, Chakravarty MM, Friedel M, Sled JG, Fletcher PJ *et al.* Adolescent Cocaine Exposure Causes Enduring Macroscale Changes in Mouse Brain Structure. *Journal of Neuroscience* 2013; **33**: 1797–1803.

53 Janes AC, Park MTM, Farmer S, Chakravarty MM. Striatal morphology is associated with tobacco cigarette craving. *Neuropsychopharmacology* 2015; **40**: 406–411.

54 Li S, Yang Y, Hoffmann E, Tyndale RF, Stein EA. CYP2A6 Genetic Variation Alters Striatal-Cingulate Circuits, Network Hubs, and Executive Processing in Smokers. *Biological Psychiatry* 2017; **81**: 554–563.

55 Terraneo A, Leggio L, Saladini M, Ermani M, Bonci A, Gallimberti L.

Transcranial magnetic stimulation of dorsolateral prefrontal cortex reduces cocaine use: A pilot study. *Eur Neuropsychopharmacol* 2016; **26**: 37–44.

56 Jaworska N, Cox SM, Casey KF, Boileau I, Cherkasova M, Larcher K *et al.* Is there a relation between novelty seeking, striatal dopamine release and frontal cortical thickness? *PLoS ONE* 2017; **12**: e0174219.

57 Volkow ND, Baler RD. Addiction science: Uncovering neurobiological complexity. *Neuropharmacology* 2014; **76**: 235–249.

58 Li Y, Yuan K, Cai C, Feng D, Yin J, Bi Y *et al.* Drug and Alcohol Dependence. *Drug Alcohol Depend* 2015; **151**: 211–219.

59 Moreno-López L, Catena A, Fernández-Serrano MJ, Delgado-Rico E, Stamatakis EA, Pérez-García M *et al.* Trait impulsivity and prefrontal gray matter reductions in cocaine dependent individuals. *Drug Alcohol Depend* 2012; **125**: 208–214.

60 Okita K, Morales AM, Dean AC, Johnson MC, Lu V, Farahi J *et al.* Striatal dopamine D1-type receptor availability: no differencefrom control but association with cortical thickness inmethamphetamine users. *Molecular psychiatry* 2017; : 1–8.

Figure Legends

Figure 1. Cortical thickness group difference.
Left column views = 1) medial, left hemisphere, 2) lateral, left hemisphere, 3) superior, 4) frontal. Right column views = 1) media, right hemisphere, 2) lateral, right hemisphere, 3) inferior, 4) occipital.

Figure 2. Scatter plot of group x age interaction in striatum volume.
HC = Healthy controls; AD = cocaine addicts. The corrected volumes are the residuals of the linear model without group and age.

Figure 3. Correlation of left nucleus accumbens and right pre-commissural putamen with cortical thickness.
Red-yellow colours show significant vertices. HC = Healthy controls, AD = cocaine addicts, lNAcc = left nucleus accumbens, rPrePut = right pre-commissural putamen. In lNAcc, for the AD group, there were were no significant peaks below FDR 5%.

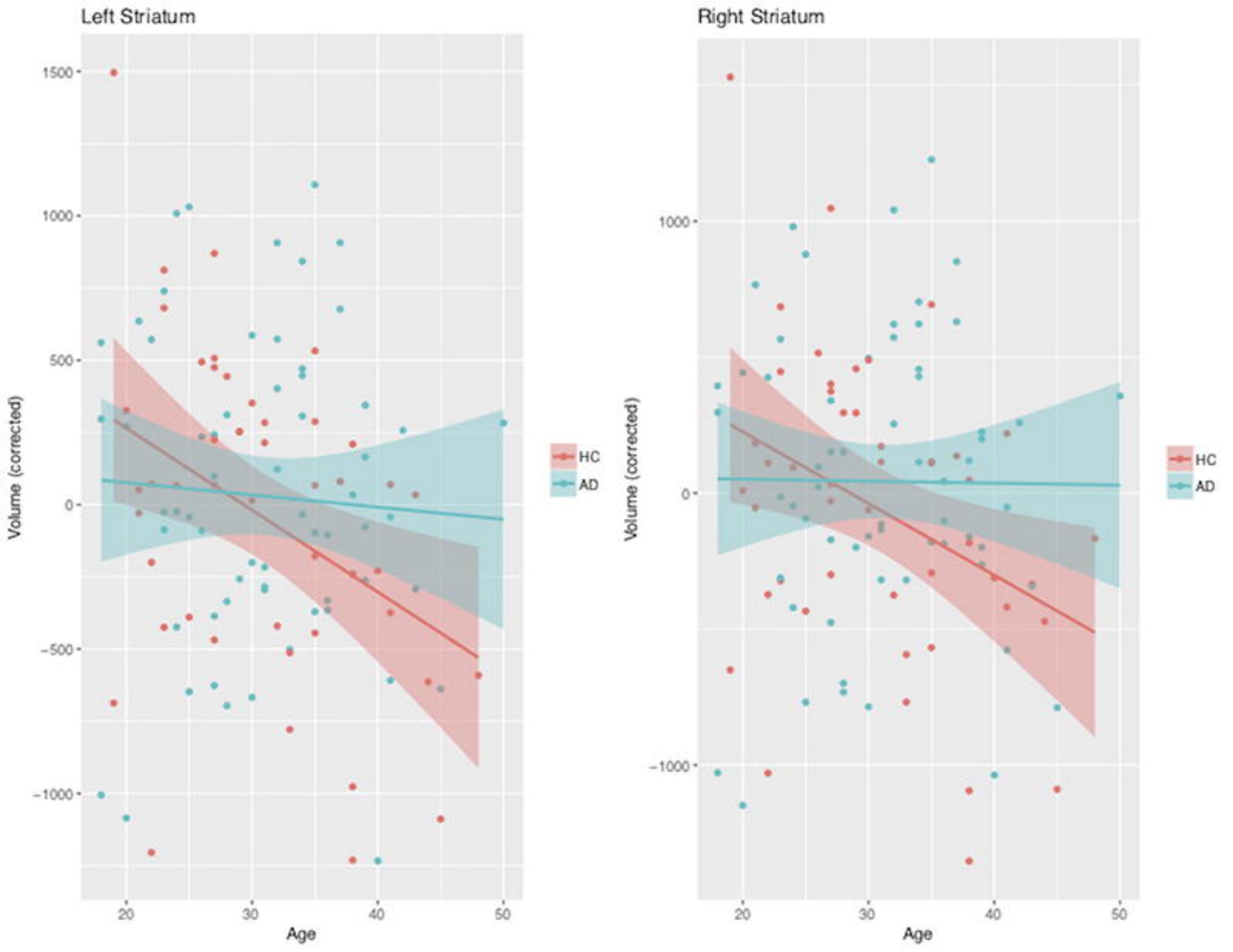
Left Striatum
Right Striatum
Volume (corrected)
Age
HC
AD
1500
1000
500
0
−500
−1000
20
30
40
50

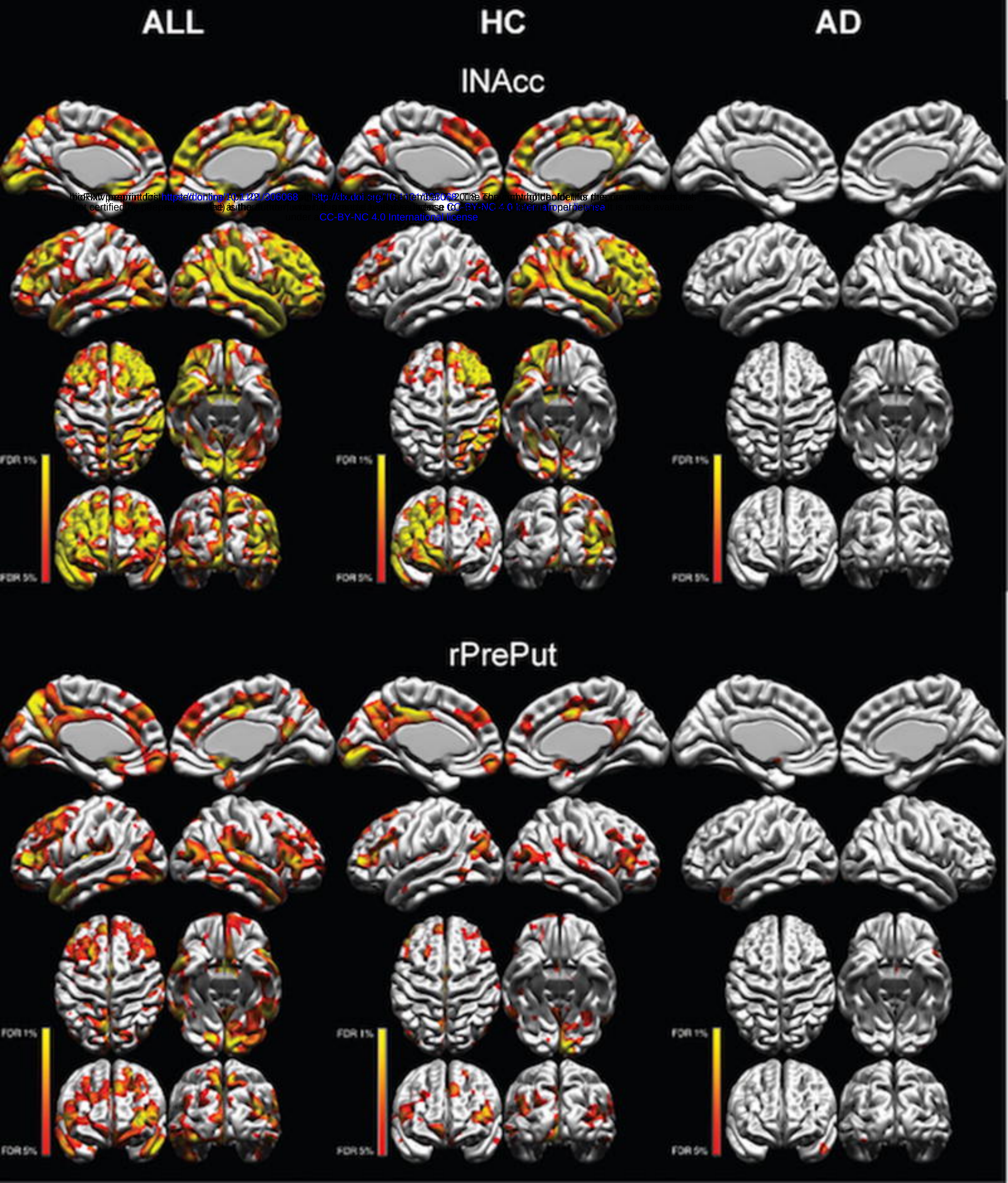

The study was approved by the local ethics committee and performed at the Instituto Nacional de Psiquiatría “Ramón de la Fuente Muñiz” in Mexico City, Mexico. The study was carried out according to the Declaration of Helsinki. Participants provided verbal and written informed consent.

Figure 1

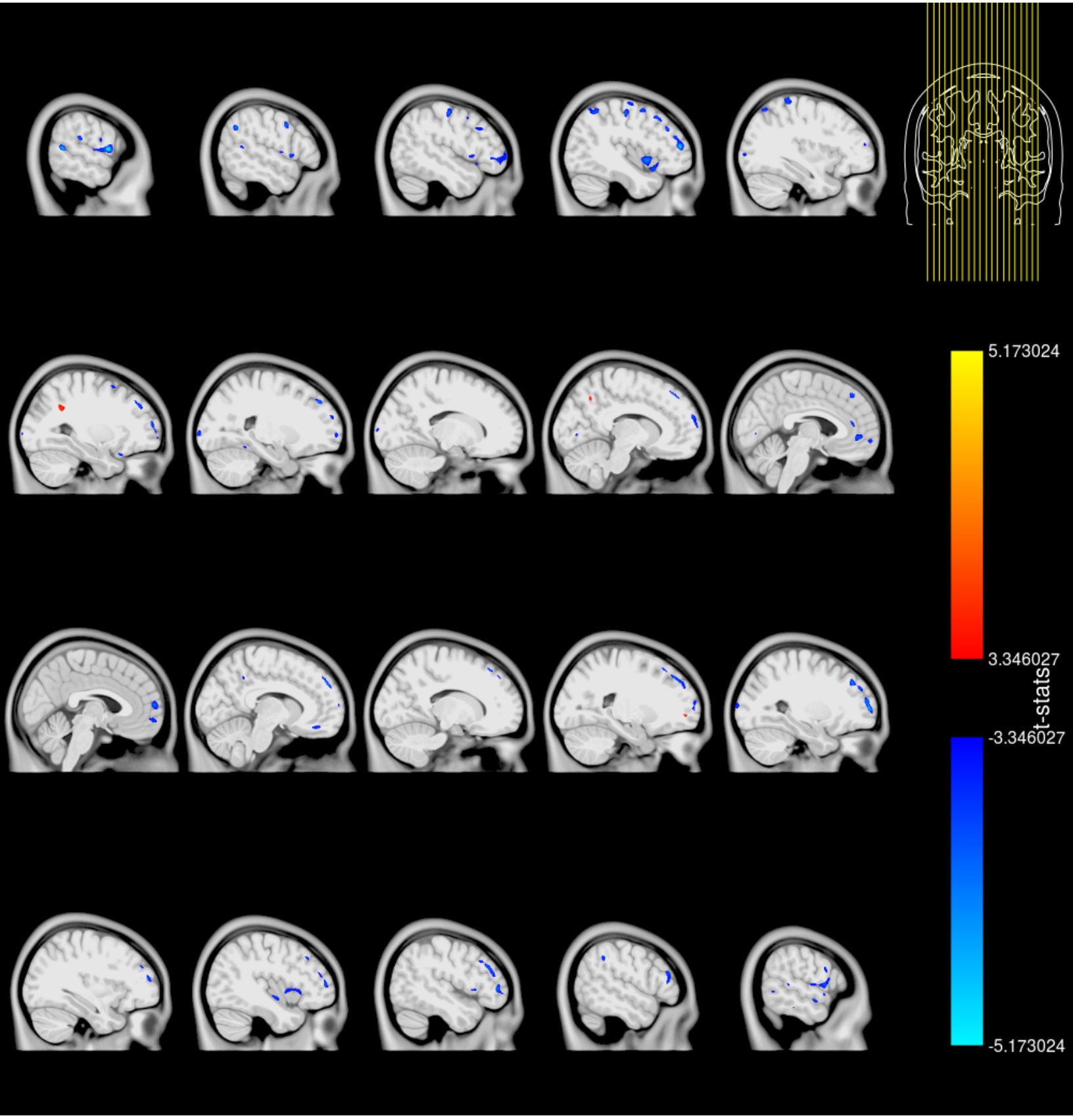

Figure 2

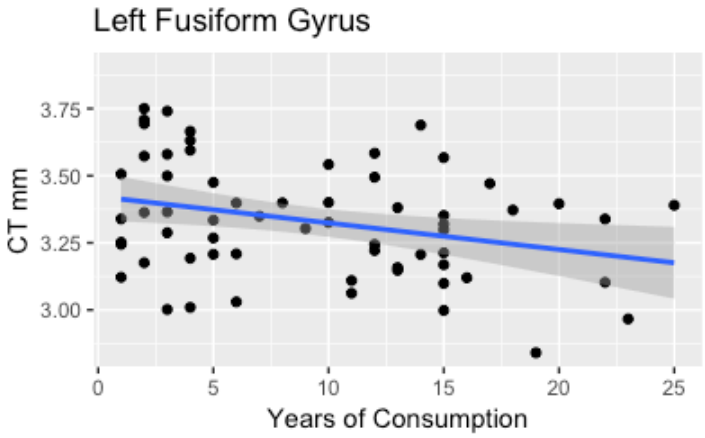

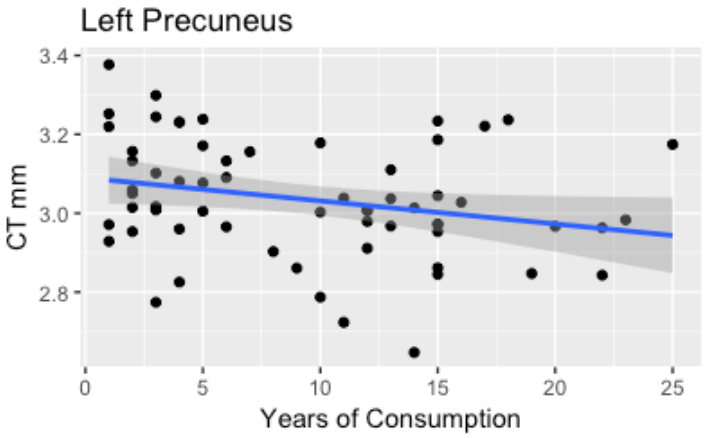

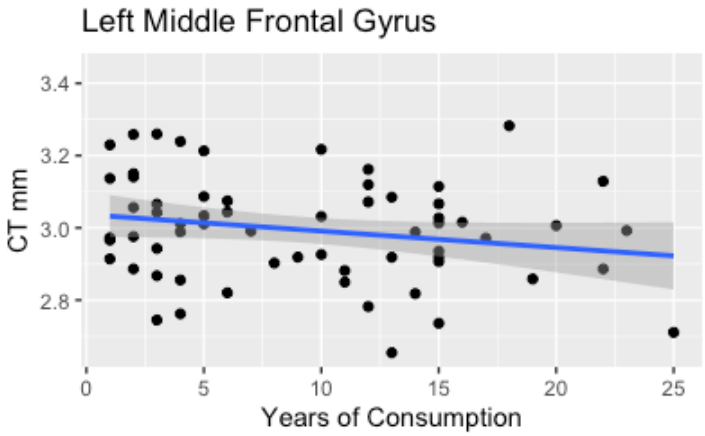

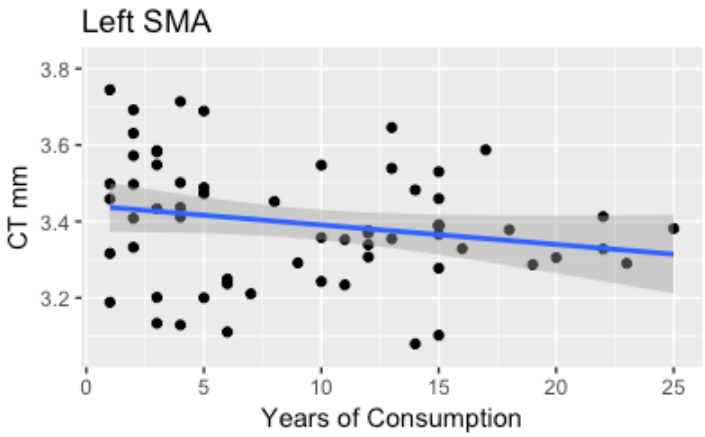

Figure 3

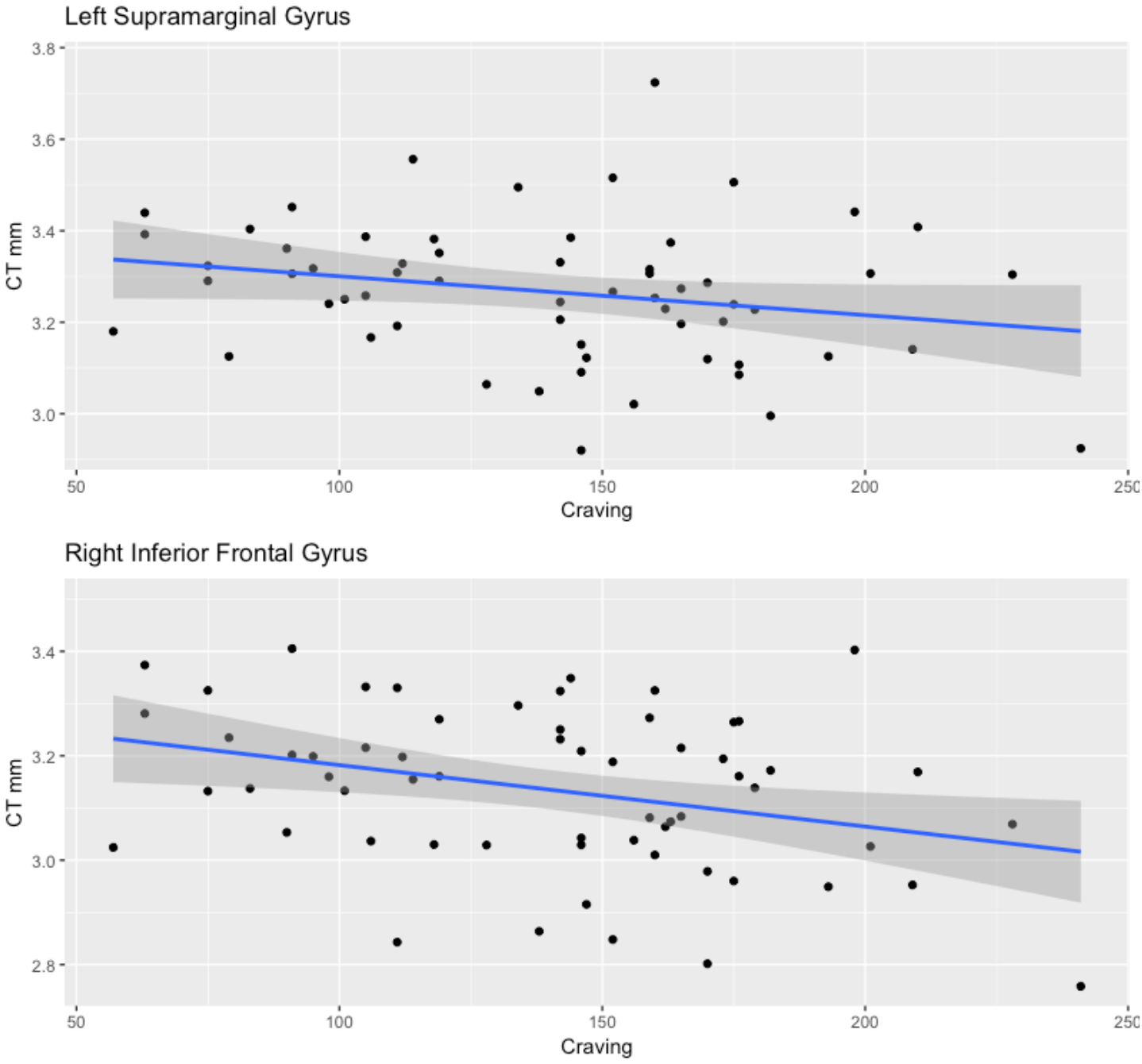

Figure 4

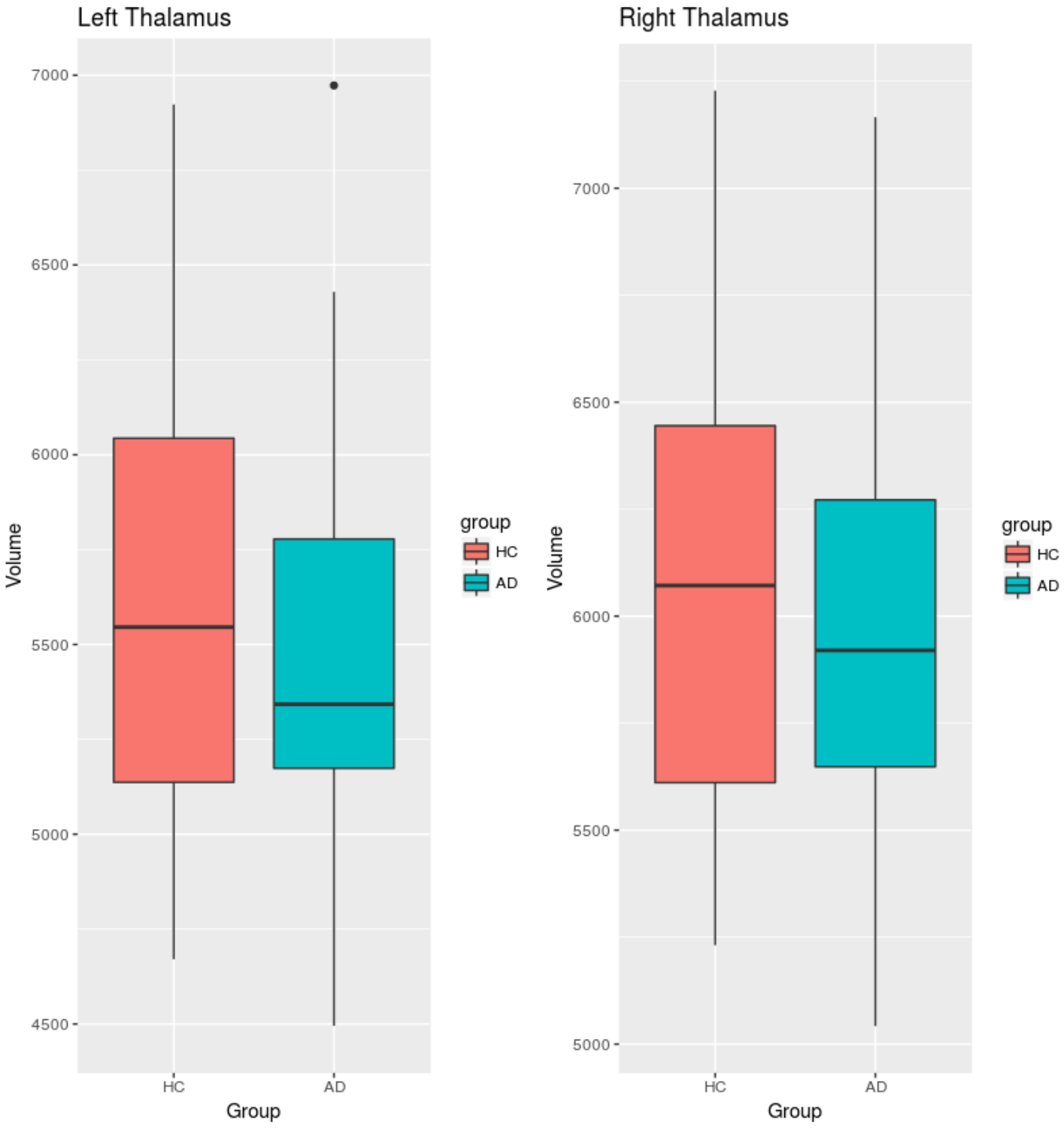

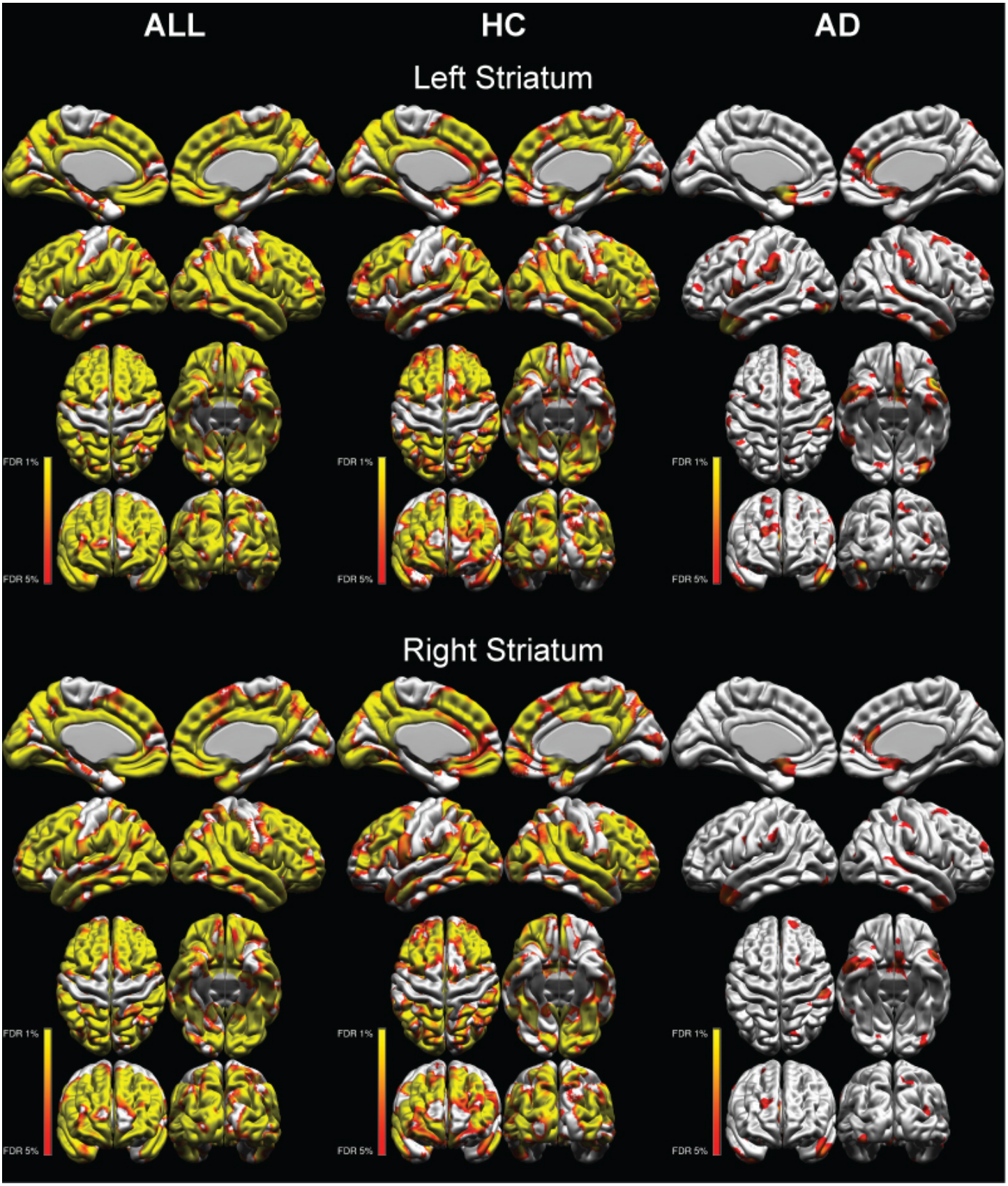

Supplementary Figure Legends

Supplementary Figure 1. Voxel-based morphometry group contrast results (CA > HC).

Supplementary Figure 2. Scatterplots between CT peaks and years of consumption.
CT = Cortical thickness.

Supplementary Figure 3. Scatterplots between CT peaks and cocaine craving.
CT = Cortical thickness.

Supplementary Figure 4. Boxplot of thalamus volume.
HC = Healthy controls, AD = Cocaine addicts.

Supplementary Figure 5. Correlation of left striatum volume and right striatum volume with cortical thickness.
HC = Healthy controls, AD = Cocaine addicts, FDR = False Discovery Rate.

Supplementary Figure Legends

Supplementary Figure 1. Voxel-based morphometry group contrast results (CA > HC).

Supplementary Figure 2. Scatterplots between CT peaks and years of consumption.
CT = Cortical thickness.

Supplementary Figure 3. Scatterplots between CT peaks and cocaine craving.
CT = Cortical thickness.

Supplementary Figure 4. Boxplot of thalamus volume.
HC = Healthy controls, AD = Cocaine addicts.

Supplementary Figure 5. Correlation of left striatum volume and right striatum volume with cortical thickness.
HC = Healthy controls, AD = Cocaine addicts, FDR = False Discovery Rate.

Supplementary Table 1. Voxel-based morphometry significant peaks.

Hem	Brain	Area				x	y	z	t
Left	Precentral	Gyrus				-60	5	9	-5.914
Left	Frontal	Pole				-43	47	12	-5.106
Left	Precentral	Gyrus				-45	-16	55	-4.813
Left	Middle	Temporal	Gyrus	temporooccipital	part	-61	-51	11	-4.763
Left	Insular	Cortex				-44	8	-6	-4.709
Left	Middle	Frontal	Gyrus			-44	31	33	-4.509
Left	Paracingulate	Gyrus				-7	24	32	-4.507
Left	Frontal	Pole				-50	37	-3	-4.469
Left	Angular	Gyrus				-54	-57	35	-4.439
Left	Frontal	Pole				-8	62	21	-4.435
Left	Superior	Frontal	Gyrus			-27	11	59	-4.385
Left	Precentral	Gyrus				-54	4	38	-4.345
Left	Middle	Frontal	Gyrus			-39	24	47	-4.322
Left	Frontal	Pole				-23	44	40	-4.319
Left	Frontal	Pole				-27	59	12	-4.252
Left	Temporal	Pole				-45	15	-11	-4.228
Left	Superior	Frontal	Gyrus			-6	40	48	-4.217
Left	Angular	Gyrus				-43	-56	53	-4.174
Left	Frontal	Pole				-9	43	47	-4.139
Left	Supramarginal	Gyrus		anterior	division	-62	-30	23	-4.122
Left	Middle	Frontal	Gyrus			-42	2	55	-4.098
Left	Frontal	Pole				-28	44	35	-4.065
Left	Middle	Frontal	Gyrus			-43	18	47	-4.047
Left	Frontal	Pole				-5	63	-7	-4.031
Left	Frontal	Pole				-49	43	-4	-4.026
Left	Paracingulate	Gyrus				-4	47	-3	-4.025
Left	Superior	Parietal	Lobule			-35	-39	67	-4.021
Left	Frontal	Pole				-41	42	24	-3.999
Left	Frontal	Pole				-24	64	0	-3.985
Left	Lateral	Occipital	Cortex	inferior	division	-36	-90	3	-3.978
Left	Lateral	Occipital	Cortex	superior	division	-35	-67	56	-3.889

Left	Occipital	Pole				-24	-102	1	-3.877
Left	Middle	Frontal	Gyrus			-47	24	35	-3.84
Left	Superior	Frontal	Gyrus			-10	38	51	-3.819
Left	Lateral	Occipital	Cortex	superior	division	-39	-63	58	-3.808
Left	Frontal	Orbital	Cortex			-29	20	-24	-3.777
Left	Frontal	Pole				-9	68	10	-3.755
Left	Frontal	Pole				-23	59	21	-3.712
Left	Frontal	Pole				-6	56	34	-3.708
Left	Precentral	Gyrus				-61	-4	20	-3.701
Left	Supramarginal	Gyrus	anterior	division		-59	-38	42	-3.658
Left	Frontal	Pole				-7	59	13	-3.647
Left	Temporal	Occipital	Fusiform			-24	-47	-15	-3.643
Left	Lingual	Gyrus				-9	-78	0	-3.637
Left	Frontal	Pole				-48	53	-1	-3.636
Left	Occipital	Pole				-15	-103	6	-3.624
Left	Cingulate	Gyrus	anterior	division		-4	40	13	-3.623
Left	Superior	Frontal	Gyrus			-6	50	28	-3.618
Left	Middle	Frontal	Gyrus			-47	7	48	-3.612
Left	Frontal	Pole				-5	59	4	-3.562
Left	Cingulate	Gyrus	anterior	division		-5	34	23	-3.516
Left	Precentral	Gyrus				-31	-12	72	-3.512
Left	Supramarginal	Gyrus	anterior	division		-51	-33	34	-3.491
Left	Cingulate	Gyrus	anterior	division		-5	35	21	-3.48
Left	Inferior	Temporal	Gyrus	temporooccipital	part	-46	-51	-22	-3.418
Left	Occipital	Pole				-26	-95	-13	-3.395
Left	Postcentral	Gyrus				-47	-29	62	-3.381
Left	Frontal	Orbital	Cortex			-38	23	-15	-3.363
Left	Precuneus	Cortex				-11	-61	44	3.808
Right	Frontal	Pole				27	61	5	-4.865
Right	Frontal	Pole				37	54	12	-4.577
Right	Inferior	Frontal	Gyrus	pars	opercularis	56	11	9	-4.537
Right	Frontal	Pole				5	62	8	-4.513
Right	Superior	Frontal	Gyrus			18	32	52	-4.482
Right	Frontal	Pole				9	54	36	-4.447

Right	Superior	Frontal	Gyrus			19	30	53	-4.441
Right	Frontal	Pole				30	56	15	-4.435
Right	Frontal	Pole				28	40	37	-4.417
Right	Frontal	Pole				25	38	44	-4.37
Right	Inferior	Frontal	Gyrus	pars	opercularis	57	13	16	-4.345
Right	Frontal	Pole				46	45	3	-4.337
Right	Middle	Frontal	Gyrus			48	31	29	-4.248
Right	Frontal	Pole				31	46	31	-4.235
Right	Frontal	Pole				45	38	23	-4.186
Right	Frontal	Pole				10	50	41	-4.169
Right	Frontal	Pole				26	50	29	-4.139
Right	Middle	Frontal	Gyrus			51	32	23	-4.129
Right	Supramarginal	Gyrus		anterior	division	63	-21	30	-4.064
Right	Middle	Frontal	Gyrus			40	30	40	-4.049
Right	Angular	Gyrus				51	-45	39	-4.023
Right	Frontal	Pole				20	50	37	-3.993
Right	Frontal	Pole				4	61	-10	-3.991
Right	Precentral	Gyrus				59	6	8	-3.976
Right	Frontal	Pole				21	47	39	-3.957
Right	Frontal	Medial	Cortex			11	41	-16	-3.944
Right	Middle	Frontal	Gyrus			46	24	37	-3.937
Right	Frontal	Operculum	Cortex			44	14	2	-3.934
Right	Occipital	Pole				27	-100	8	-3.883
Right	Precentral	Gyrus				60	7	25	-3.882
Right	Central	Opercular	Cortex			58	-8	8	-3.873
Right	Frontal	Pole				45	49	-2	-3.864
Right	Middle	Temporal	Gyrus	anterior	division	60	-5	-12	-3.843
Right	Planum	Polare				42	-9	-8	-3.825
Right	Superior	Temporal	Gyrus	posterior	division	64	-36	8	-3.802
Right	Precuneous	Cortex				7	-48	43	-3.8
Right	Frontal	Pole				0	60	-9	-3.776
Right	Inferior	Frontal	Gyrus	pars	triangularis	54	32	11	-3.762
Right	Inferior	Frontal	Gyrus	pars	triangularis	53	34	14	-3.757
Right	Frontal	Pole				6	58	18	-3.73

Right	Frontal	Pole				23	65	13	-3.722
Right	Inferior	Frontal	Gyrus	pars	opercularis	56	21	10	-3.643
Right	Frontal	Operculum	Cortex			41	21	-2	-3.587
Right	Occipital	Fusiform	Gyrus			20	-72	-11	-3.578
Right	Middle	Temporal	Gyrus	posterior	division	69	-10	-19	-3.571
Right	Middle	Temporal	Gyrus	temporooccipital	part	60	-56	-1	-3.56
Right	Postcentral	Gyrus				43	-21	51	-3.504
Right	Precentral	Gyrus				56	-1	40	-3.494
Right	Superior	Temporal	Gyrus	anterior	division	59	6	-4	-3.492
Right	Inferior	Temporal	Gyrus	posterior	division	59	-31	-20	-3.43
Right	Postcentral	Gyrus				43	-22	65	-3.413
Right	Lateral	Occipital	Cortex	inferior	division	39	-90	-4	-3.403
Right	Frontal	Pole				45	56	-13	-3.374
Right	Precentral	Gyrus				4	-21	54	-3.349
Right	Temporal	Pole				42	11	-16	-3.347
Right	Frontal	Pole				21	54	-3	3.644

Hem = Hemisphere, t = t-value, coordinates are in MNI.

Supplementary Table 2. Cortical thickness significant peaks at FDR 10%.

Brain Areas	vertex	x	y	z	t
Left Superior frontal gyrus, medial orbital	17449	-2	63	-6	-4.31
Left Postcentral gyrus	21560	-60	2	15	-4.14
Left Rolandic operculum	21525	-60	4	14	-4.03
Left Precentral gyrus	21506	-61	2	19	-3.95
Left Superior frontal gyrus, dorsolateral	4509	-25	56	23	-3.93
Left Superior frontal gyrus, medial	27538	-13	56	33	-3.76
Left Middle temporal gyrus	22615	-53	-48	14	-3.61
Left Inferior frontal gyrus, orbital part	3138	-38	37	-15	-3.6
Left Fusiform gyrus	36594	-40	-10	-35	-3.53
Left Middle frontal gyrus	18317	-37	53	22	-3.52
Left Inferior temporal gyrus	36593	-40	-9	-35	-3.5
Left Superior temporal gyrus	22591	-57	-51	18	-3.46
Left Supplementary motor area	7066	-2	30	49	-3.34
Left Middle occipital gyrus	33739	-49	-82	-4	-3.28
Left Inferior occipital gyrus	35976	-53	-61	-11	-3.28
Left Precuneus	31415	-7	-59	53	-3.22
Left Gyrus Rectus	16957	-2	62	-15	-3.21
Left Median cingulate and paracingulate gyri	28377	-8	13	39	-3.17
Left Calcarine fissure and surrounding cortex	33121	-11	-106	-1	-3.1
Left Angular gyrus	23260	-51	-54	28	-3
Left Cuneus	38907	-20	-51	0	-2.98
Left Inferior frontal gyrus, triangular part	19006	-40	44	8	-2.93
Left Supramarginal gyrus	22145	-56	-20	22	-2.83
Left Supeiror frontal gyrus, orbital part	15296	-13	23	-20	-2.81
Left Parahippocampal gyrus	14365	-25	2	-25	-2.81
Left Lingual gyrus	2449	-20	-51	0	-2.77
Left Inferior frontal gyrus, opercular part	19986	-56	22	16	-2.76
Left Insula	10363	-43	-6	-2	-2.73
Left Temporal pole: superior temporal gyrus	14236	-23	4	-27	-2.71
Left Olfactory Cortex	16118	-16	6	-19	-2.62

Left Superior parietal gyrus	25046	-22	-40	64	-2.57
Left Anterior cingulate and paracingulate gyri	28577	-7	19	34	-2.56
Left Superior occipital gyrus	2121	-25	-96	4	-2.48
Left Middle frontal gyrus orbital part	19068	-44	51	1	-2.46
Left Paracentral lobule	30828	-3	-36	54	-2.44
Right Superior frontal gyrus, medial orbital	17449	-2	63	-6	-4.31
Right Rolandic operculum	21560	-60	2	15	-4.14
Right Precentral gyrus	21506	-61	2	19	-3.95
Right Superior frontal gyrus, dorsolateral	4509	-25	56	23	-3.93
Right Superior frontal gyrus, medial	17540	-3	65	-4	-3.91
Right Postcentral gyrus	5410	-60	0	19	-3.83
Right Middle frontal gyrus	4523	-24	51	21	-3.81
Right Superior temporal gyrus	22615	-53	-48	14	-3.61
Right Inferior frontal gyrus, orbital part	3138	-38	37	-15	-3.6
Right Middle temporal gyrus	36414	-52	-53	13	-3.6
Right Fusiform gyrus	36594	-40	-10	-35	-3.53
Right Inferior temporal gyrus	36593	-40	-9	-35	-3.5
Right Middle occipital gyrus	33739	-49	-82	-4	-3.28
Right Precuneus	31415	-7	-59	53	-3.22
Right Median cingulate and paracingulate gyri	28373	-8	14	39	-3.18
Right Gyrus Rectus	16956	-2	63	-17	-3.14
Right Calcarine fissure and surrounding cortex	33121	-11	-106	-1	-3.1
Right Supplementary motor area	28356	-7	15	39	-3.09
Right Inferior occipital gyrus	8459	-46	-80	-7	-3.04
Right Cuneus	38907	-20	-51	0	-2.98
Right Angular gyrus	23257	-50	-54	29	-2.96
Right Inferior frontal gyrus, triangular part	19006	-40	44	8	-2.93
Right Superior parietal gyrus	25062	-18	-40	72	-2.93
Right Supramarginal gyrus	22145	-56	-20	22	-2.83
Right Superior frontal gyrus, orbital part	15296	-13	23	-20	-2.81
Right Parahippocampal gyrus	14247	-24	2	-26	-2.81
Right Temporal pole: superior temporal gyrus	14365	-25	2	-25	-2.81
Right Lingual gyrus	2449	-20	-51	0	-2.77
Right Inferior frontal gyrus, opercular part	19986	-56	22	16	-2.76

Right Insula	10363	-43	-6	-2	-2.73
Right Olfactory Cortex	16118	-16	6	-19	-2.62

Vertex = vertex peak in MINC format, t = t-value. Coordinates in MNI.

Supplementary Table 3. Correlations between CT peaks and years of cocaine use.

Brain Area	vertex	r	uncorr-p	fdr-p
Left Fusiform Gyrus	36594	-0.35	0.003	0.02
Left Middle Frontal Gyrus	18317	-0.20	0.057	0.057
Left SMA	7066	-0.24	0.031	0.05
Left Precuneus	31415	-0.22	0.047	0.057
Left Insula	10363	-0.26	0.023	0.046

Vertex = Surface vertex CIVET 1.1.12, r = correlation coefficient, uncorr-p = non-corrected p value, fdr-p = p value corrected for multiple comparisons using false discovery rate.

Supplementary Table 4. Correlations between CT peaks and cocaine craving.

Brain Area	vertex	r	uncorr-p	fdr-p
Left Supramarginal Gyrus	22145	-0.24	0.034	0.045
Right Middle Frontal Gyrus	18285	-0.22	0.042	0.045
Right Lingual Gyrus	9552	-0.22	0.045	0.045
Right Parahippocampal Gyrus	38137	-0.24	0.033	0.045

Vertex = Surface vertex CIVET 1.1.12, r = correlation coefficient, uncorr-p = non-corrected p value, fdr-p = p value corrected for multiple comparisons using false discovery rate.

Supplementary Table 5. Left Striatum volume significant peaks of correlation with cortical thickness in ALL participants.

Brain Area	vertex	x	y	z	t
Left Calcarine fissure and surrounding cortex	33295	-11	-92	-19	6
Left Olfactory Cortex	4040	-2	17	-14	5.96
Left Lingual gyrus	39387	-12	-87	-20	5.91
Left Middle temporal gyrus	13331	-53	12	-30	5.61
Left Anterior cingulate and paracingulate gyri	16051	-3	20	-13	5.59
Left Superior temporal gyrus	22384	-45	-34	17	5.5
Left Gyrus Rectus	15115	-6	39	-28	5.39
Left Inferior occipital gyrus	33480	-34	-90	-10	5.3
Left Precuneus	40676	-13	-52	2	5.3
Left Superior frontal gyrus, medial orbital	15921	-5	25	-14	5.29
Left Middle occipital gyrus	33446	-33	-93	-10	5.23
Left Supramarginal gyrus	22244	-43	-33	16	5.11
Left Rolandic operculum	5493	-37	-26	19	5.07
Left Fusiform gyrus	35422	-40	-75	-16	5.01
Left Heschl gyrus	672	-39	-31	18	5.01
Left Temporal pole: superior temporal gyrus	13189	-50	16	-29	5
Left Temporal pole: middle temporal gyrus	3348	-49	14	-32	4.99

Left Insula	10525	-39	-17	5	4.97
Left Precentral gyrus	20887	-53	-5	30	4.96
Left Inferior frontal gyrus, opercular part	20608	-40	12	28	4.96
Left Angular gyrus	23649	-48	-48	49	4.96
Left Middle frontal gyrus	20597	-39	11	28	4.94
Left Inferior frontal gyrus, triangular part	20611	-41	12	28	4.93
Left Cuneus	38388	-15	-55	4	4.91
Left Superior frontal gyrus, dorsolateral	6720	-23	-5	55	4.89
Left Inferior parietal, but supramarginal and angular gyri	23531	-47	-47	47	4.75
Left Median cingulate and paracingulate gyri	7483	-5	-18	44	4.66
Left Postcentral gyrus	20865	-53	-6	29	4.66
Left Supplementary motor area	1772	-8	3	45	4.54
Left Superior frontal gyrus, medial	28049	-4	42	35	4.32
Left Posterior cingulate gyrus	40909	-2	-52	16	4.31
Left Superior occipital gyrus	33893	-27	-85	21	4.28
Left Inferior temporal gyrus	36703	-45	-24	-26	4.17
Left Superior parietal gyrus	25063	-29	-40	59	4.13
Left Middle frontal gyrus orbital part	19079	-42	52	1	4.1
Left Supeiror frontal gyrus, orbital part	15206	-10	40	-23	3.88

Left Paracentral lobule	30979	-13	-44	62	3.79
Left Parahippocampal gyrus	37578	-30	-50	-8	3.57
Left Inferior frontal gyrus, orbital part	18643	-39	52	-13	3.45
Right Rolandic operculum	21843	-40	-24	18	6.22
Right Superior temporal gyrus	13008	-45	-2	-11	6.02
Right Anterior cingulate and paracingulate gyri	16045	-3	16	-14	5.99
Right Supramarginal gyrus	21832	-42	-25	19	5.97
Right Inferior frontal gyrus, triangular part	19447	-42	22	7	5.8
Right Olfactory Cortex	16042	-3	15	-15	5.79
Right Heschl gyrus	10642	-40	-30	15	5.79
Right Insula	10569	-36	-23	16	5.73
Right Middle occipital gyrus	34433	-41	-88	13	5.65
Right Median cingulate and paracingulate gyri	29837	-11	-21	41	5.58
Right Postcentral gyrus	21790	-47	-16	15	5.52
Right Temporal pole: superior temporal gyrus	3279	-45	5	-14	5.47
Right Superior frontal gyrus, medial	4440	-4	52	25	5.4
Right Inferior frontal gyrus, opercular part	19526	-42	20	7	5.39
Right Middle temporal gyrus	11030	-55	-18	-8	5.36
Right Superior occipital gyrus	34019	-26	-84	18	5.26

Right Posterior cingulate gyrus	30208	-7	-51	32	5.21
Right Inferior parietal, but supramarginal and angular gyri	22744	-49	-31	44	5.18
Right Temporal pole: middle temporal gyrus	3374	-53	9	-39	5.18
Right Lingual gyrus	39369	-15	-82	-18	5.14
Right Precuneus	7934	-10	-76	50	5.14
Right Supeiror frontal gyrus, orbital part	888	-24	29	-20	5.06
Right Superior parietal gyrus	31649	-11	-74	50	5.01
Right Supplementary motor area	7030	-9	-1	46	4.94
Right Middle frontal gyrus	19788	-33	38	31	4.9
Right Superior frontal gyrus, medial orbital	4028	-2	20	-17	4.84
Right Inferior temporal gyrus	856	-47	2	-41	4.8
Right Inferior frontal gyrus, orbital part	13926	-24	28	-18	4.71
Right Precentral gyrus	20657	-44	9	24	4.66
Right Superior frontal gyrus, dorsolateral	27336	-18	54	37	4.62
Right Cuneus	31915	-17	-67	20	4.33
Right Angular gyrus	24041	-28	-67	33	4.32
Right Calcarine fissure and surrounding cortex	39388	-9	-86	-18	4.24
Right Fusiform gyrus	37897	-25	-76	-13	4.21
Right Gyrus Rectus	3841	-11	28	-23	4.2

Right Paracentral lobule	1862	-9	-26	46	3.98
Right Middle frontal gyrus orbital part	18535	-23	54	-15	3.79
Right Inferior occipital gyrus	33607	-35	-91	-7	3.78
Right Parahippocampal gyrus	14247	-24	2	-26	3.65

Supplementary Table 6. Right Striatum volume significant peaks of correlation with cortical thickness in ALL participants.

Brain Area	**vertex**	**x**	**y**	**z**	**t**
Left Calcarine fissure and surrounding cortex	33295	-11	-92	-19	6.02
Left Olfactory Cortex	16045	-3	16	-14	5.9
Left Lingual gyrus	39387	-12	-87	-20	5.84
Left Anterior cingulate and paracingulate gyri	16051	-3	20	-13	5.33
Left Precuneus	10176	-12	-52	3	5.29
Left Superior frontal gyrus, medial orbital	16931	-4	57	-14	5.25
Left Middle temporal gyrus	13331	-53	12	-30	5.22
Left Gyrus Rectus	16932	-3	58	-15	5.16
Left Superior temporal gyrus	22384	-45	-34	17	4.98
Left Insula	10525	-39	-17	5	4.96
Left Middle occipital gyrus	537	-33	-92	-10	4.93
Left Inferior occipital gyrus	33480	-34	-90	-10	4.93

Left Rolandic operculum	21836	-40	-25	19	4.86
Left Supramarginal gyrus	21837	-40	-26	20	4.85
Left Cuneus	9619	-14	-56	5	4.83
Left Angular gyrus	23649	-48	-48	49	4.8
Left Fusiform gyrus	35422	-40	-75	-16	4.78
Left Inferior frontal gyrus, triangular part	11869	-32	21	11	4.76
Left Temporal pole: superior temporal gyrus	13188	-49	16	-30	4.75
Left Inferior frontal gyrus, opercular part	20608	-40	12	28	4.73
Left Middle frontal gyrus	20597	-39	11	28	4.72
Left Heschl gyrus	2642	-39	-19	4	4.69
Left Temporal pole: middle temporal gyrus	3348	-49	14	-32	4.65
Left Precentral gyrus	26764	-23	-5	54	4.58
Left Superior frontal gyrus, dorsolateral	26745	-23	-4	54	4.58
Left Inferior parietal, but supramarginal and angular gyri	23531	-47	-47	47	4.56
Left Median cingulate and paracingulate gyri	29812	-4	-19	44	4.5
Left Postcentral gyrus	22201	-48	-23	19	4.48
Left Posterior cingulate gyrus	40909	-2	-52	16	4.46
Left Superior occipital gyrus	33893	-27	-85	21	4.37
Left Inferior temporal gyrus	36703	-45	-24	-26	4.16

Left Superior frontal gyrus, medial	7043	-5	43	34	4.1
Left Supplementary motor area	1772	-8	3	45	4.06
Left Superior parietal gyrus	23435	-32	-55	43	3.97
Left Middle frontal gyrus orbital part	18981	-33	58	3	3.78
Left Supeiror frontal gyrus, orbital part	15200	-11	37	-23	3.71
Left Paracentral lobule	30979	-13	-44	62	3.45
Left Parahippocampal gyrus	37578	-30	-50	-8	3.4
Left Inferior frontal gyrus, orbital part	18643	-39	52	-13	3.19
Right Anterior cingulate and paracingulate gyri	16045	-3	16	-14	6.17
Right Olfactory Cortex	16042	-3	15	-15	5.99
Right Rolandic operculum	21843	-40	-24	18	5.98
Right Middle occipital gyrus	34433	-41	-88	13	5.86
Right Supramarginal gyrus	21837	-40	-26	20	5.77
Right Superior temporal gyrus	13008	-45	-2	-11	5.68
Right Median cingulate and paracingulate gyri	29682	-2	-2	44	5.59
Right Heschl gyrus	10639	-39	-30	17	5.59
Right Inferior frontal gyrus, triangular part	19447	-42	22	7	5.57
Right Insula	10569	-36	-23	16	5.47
Right Superior occipital gyrus	34019	-26	-84	18	5.28

Right Inferior frontal gyrus, opercular part	19526	-42	20	7	5.19
Right Postcentral gyrus	21790	-47	-16	15	5.12
Right Lingual gyrus	39369	-15	-82	-18	5.06
Right Supeiror frontal gyrus, orbital part	888	-24	29	-20	5.05
Right Superior frontal gyrus, medial	4440	-4	52	25	5.04
Right Middle temporal gyrus	9114	-54	-50	11	5.03
Right Temporal pole: superior temporal gyrus	3279	-45	5	-14	4.99
Right Inferior parietal, but supramarginal and angular gyri	22744	-49	-31	44	4.97
Right Supplementary motor area	7030	-9	-1	46	4.95
Right Precuneus	7934	-10	-76	50	4.93
Right Superior parietal gyrus	31655	-12	-74	50	4.9
Right Posterior cingulate gyrus	30152	-4	-52	26	4.88
Right Temporal pole: middle temporal gyrus	3374	-53	9	-39	4.88
Right Superior frontal gyrus, medial orbital	15996	-1	18	-17	4.82
Right Middle frontal gyrus	19788	-33	38	31	4.6
Right Inferior frontal gyrus, orbital part	13923	-24	27	-19	4.59
Right Inferior temporal gyrus	856	-47	2	-41	4.42
Right Superior frontal gyrus, dorsolateral	27336	-18	54	37	4.39
Right Precentral gyrus	20651	-44	9	25	4.36

Right Cuneus	31915	-17	-67	20	4.19
Right Fusiform gyrus	9422	-35	-54	-19	4.16
Right Angular gyrus	24041	-28	-67	33	4.15
Right Calcarine fissure and surrounding cortex	39388	-9	-86	-18	4.05
Right Gyrus Rectus	3841	-11	28	-23	4.02
Right Paracentral lobule	1862	-9	-26	46	3.91
Right Inferior occipital gyrus	33607	-35	-91	-7	3.85
Right Middle frontal gyrus orbital part	18538	-23	51	-14	3.74
Right Parahippocampal gyrus	14247	-24	2	-26	3.55

Supplementary Table 7. Left Striatum volume significant peaks of correlation with cortical thickness in HC.

Brain Areas	**vertex**	**x**	**y**	**z**	**t**
Left Calcarine fissure and surrounding cortex	33295	-11	-92	-19	5.93
Left Precuneus	30271	-1	-61	23	5.73
Left Lingual gyrus	39387	-12	-87	-20	5.69
Left Inferior frontal gyrus, triangular part	19963	-44	29	22	5.6
Left Superior frontal gyrus, medial orbital	16899	-5	56	-14	5.55
Left Median cingulate and paracingulate gyri	30717	-5	-41	48	5.44
Left Inferior frontal gyrus, opercular part	20043	-50	13	24	5.26

Left Middle frontal gyrus	20500	-44	21	28	5.25
Left Middle occipital gyrus	8937	-44	-67	-4	4.97
Left Gyrus Rectus	4261	-4	56	-15	4.94
Left Inferior occipital gyrus	35622	-45	-66	-5	4.88
Left Fusiform gyrus	9424	-37	-57	-20	4.82
Left Supplementary motor area	27985	-5	4	47	4.68
Left Superior parietal gyrus	25164	-23	-41	63	4.61
Left Superior frontal gyrus, dorsolateral	26093	-21	27	59	4.54
Left Precentral gyrus	20657	-44	9	24	4.49
Left Superior temporal gyrus	22415	-51	-36	20	4.34
Left Postcentral gyrus	25162	-21	-42	64	4.3
Left Superior frontal gyrus, medial	444	-8	53	43	4.24
Left Posterior cingulate gyrus	30229	-3	-53	19	4.23
Left Supramarginal gyrus	22367	-51	-38	24	4.2
Left Superior occipital gyrus	32420	-29	-86	29	4.18
Left Middle temporal gyrus	34871	-51	-55	15	4.18
Left Cuneus	9614	-18	-53	1	4.14
Left Angular gyrus	5941	-45	-48	47	4.05
Left Insula	664	-39	-18	6	4.04

Left Inferior temporal gyrus	35914	-61	-56	-8	3.99
Left Inferior parietal, but supramarginal and angular gyri	23644	-45	-47	46	3.98
Left Rolandic operculum	21781	-39	-12	18	3.97
Left Heschl gyrus	2642	-39	-19	4	3.92
Left Olfactory Cortex	16045	-3	16	-14	3.88
Left Anterior cingulate and paracingulate gyri	15430	-5	25	-14	3.82
Left Middle frontal gyrus orbital part	4774	-37	58	3	3.81
Left Paracentral lobule	30989	-13	-44	64	3.69
Left Superior frontal gyrus, orbital part	15206	-10	40	-23	3.18
Left Parahippocampal gyrus	3614	-27	0	-23	3
Left Temporal pole: superior temporal gyrus	13149	-44	15	-19	2.99
Left Inferior frontal gyrus, orbital part	4808	-42	46	-2	2.88
Left Temporal pole: middle temporal gyrus	3340	-48	12	-30	2.66
Right Median cingulate and paracingulate gyri	1850	-10	-18	44	6.31
Right Posterior cingulate gyrus	30084	-8	-48	36	5.92
Right Supplementary motor area	27967	-6	-3	47	5.81
Right Middle frontal gyrus	18329	-34	43	28	5.74
Right Anterior cingulate and paracingulate gyri	28019	-4	48	27	5.72
Right Superior temporal gyrus	2732	-62	-9	-4	5.69

Right Paracentral lobule	29429	-8	-25	46	5.67
Right Superior frontal gyrus, medial	27624	-4	50	28	5.64
Right Supramarginal gyrus	22224	-45	-29	16	5.61
Right Precuneus	30434	-9	-52	35	5.53
Right Inferior frontal gyrus, triangular part	19399	-54	32	9	5.4
Right Middle occipital gyrus	34407	-43	-83	13	5.36
Right Superior frontal gyrus, orbital part	13954	-23	36	-24	5.17
Right Rolandic operculum	21834	-43	-24	19	5.02
Right Heschl gyrus	11075	-44	-30	11	5
Right Olfactory Cortex	16042	-3	15	-15	4.97
Right Middle temporal gyrus	10914	-55	-5	-14	4.93
Right Superior occipital gyrus	34045	-31	-77	20	4.85
Right Lingual gyrus	39373	-14	-83	-18	4.83
Right Superior frontal gyrus, medial orbital	17547	-7	72	-6	4.74
Right Insula	2591	-38	-11	16	4.71
Right Superior frontal gyrus, dorsolateral	18009	-25	52	34	4.68
Right Parahippocampal gyrus	915	-27	2	-23	4.68
Right Postcentral gyrus	22201	-48	-23	19	4.56
Right Inferior occipital gyrus	8436	-39	-90	-4	4.5

Right Temporal pole: superior temporal gyrus	14405	-27	3	-23	4.4
Right Inferior frontal gyrus, orbital part	4856	-47	33	-4	4.36
Right Fusiform gyrus	9348	-36	-50	-20	4.32
Right Middle frontal gyrus orbital part	4671	-29	54	-17	4.29
Right Inferior parietal, but supramarginal and angular gyri	5892	-43	-45	43	4.27
Right Inferior frontal gyrus, opercular part	20620	-43	11	26	4.25
Right Superior parietal gyrus	25245	-27	-57	66	4.19
Right Cuneus	38474	-16	-60	10	4.13
Right Angular gyrus	5611	-62	-51	33	4.13
Right Inferior temporal gyrus	36752	-44	-26	-22	4.13
Right Gyrus Rectus	15270	-11	27	-23	3.87
Right Precentral gyrus	20242	-47	10	21	3.84
Right Calcarine fissure and surrounding cortex	9864	-11	-88	-20	3.82
Right Temporal pole: middle temporal gyrus	3374	-53	9	-39	3.8

Supplementary Table 8. Left Striatum volume significant peaks of correlation with cortical thickness in AD.

Brain Areas	**vertex**	**x**	**y**	**z**	**t**
Left Temporal pole: middle temporal gyrus	13483	-47	18	-35	4.85
Left Temporal pole: superior temporal gyrus	13482	-47	18	-34	4.83

Left Middle temporal gyrus	13321	-51	14	-32	4.82
Left Inferior occipital gyrus	33470	-36	-88	-17	4.77
Left Olfactory Cortex	16046	-3	15	-13	4.75
Left Precentral gyrus	5246	-54	-5	30	4.53
Left Anterior cingulate and paracingulate gyri	16057	-2	17	-11	4.47
Left Superior temporal gyrus	13025	-45	1	-13	4.42
Left Postcentral gyrus	5245	-54	-5	28	4.33
Left Gyrus Rectus	15776	-11	19	-23	3.94
Left Rolandic operculum	5063	-54	9	-1	3.91
Left Middle occipital gyrus	33487	-37	-89	-10	3.84
Left Inferior frontal gyrus, opercular part	20117	-51	10	-2	3.81
Left Superior frontal gyrus, medial orbital	15918	-4	25	-15	3.76
Left Fusiform gyrus	35425	-37	-77	-15	3.73
Left Supramarginal gyrus	22112	-59	-20	27	3.7
Left Inferior frontal gyrus, triangular part	11934	-32	26	8	3.59
Left Superior frontal gyrus, dorsolateral	26709	-24	0	59	3.49
Left Heschl gyrus	10647	-41	-32	14	3.45
Left Inferior temporal gyrus	36527	-45	-6	-47	3.41
Left Lingual gyrus	35451	-33	-81	-18	3.37

Left Insula	3193	-42	-3	-12	3.34
Left Precuneus	40677	-13	-53	3	3.33
Left Inferior parietal, but supramarginal and angular gyri	21485	-62	-34	41	3.31
Left Angular gyrus	23649	-48	-48	49	3.29
Left Cuneus	38388	-15	-55	4	3.22
Left Middle frontal gyrus	1213	-40	49	8	3.15
Left Inferior frontal gyrus, orbital part	18773	-46	49	-13	3.05
Left Calcarine fissure and surrounding cortex	32853	-2	-85	17	3.02
Right Anterior cingulate and paracingulate gyri	16540	-1	38	12	5.06
Right Supramarginal gyrus	5387	-52	-29	43	4.56
Right Superior temporal gyrus	13011	-45	-1	-11	4.52
Right Temporal pole: superior temporal gyrus	13032	-44	4	-15	4.47
Right Temporal pole: middle temporal gyrus	13635	-43	8	-42	4.42
Right Inferior parietal, but supramarginal and angular gyri	22732	-47	-30	42	4.35
Right Inferior temporal gyrus	13600	-41	8	-44	4.31
Right Middle temporal gyrus	13438	-55	4	-35	4.19
Right Postcentral gyrus	22857	-42	-30	41	4.01
Right Inferior frontal gyrus, triangular part	19502	-40	20	7	3.98
Right Rolandic operculum	5488	-37	-23	18	3.96

Right Inferior frontal gyrus, opercular part	19526	-42	20	7	3.94
Right Insula	10569	-36	-23	16	3.77
Right Superior frontal gyrus, dorsolateral	17856	-18	58	26	3.74
Right Heschl gyrus	10628	-36	-28	18	3.7
Right Superior frontal gyrus, medial orbital	4031	-3	22	-16	3.59
Right Olfactory Cortex	15994	-2	16	-16	3.52
Right Superior parietal gyrus	24343	-38	-39	58	3.51
Right Precuneus	30663	-9	-73	34	3.51
Right Superior frontal gyrus, medial	17716	-14	61	26	3.49
Right Middle occipital gyrus	8639	-37	-88	16	3.42
Right Lingual gyrus	39399	-20	-79	-17	3.31
Right Fusiform gyrus	8855	-47	-47	-17	3.29
Right Inferior frontal gyrus, orbital part	13923	-24	27	-19	3.18
Right Precentral gyrus	20663	-45	9	24	3.16
Right Superior frontal gyrus, orbital part	13927	-24	28	-19	3.16
Right Middle frontal gyrus	26755	-23	4	56	3.14
Right Superior occipital gyrus	2097	-24	-100	-4	3.08
Right Median cingulate and paracingulate gyri	28625	-8	29	28	2.99
Right Supplementary motor area	26876	-13	22	59	2.98

Right Calcarine fissure and surrounding cortex	39255	-8	-79	-11	2.94
Right Cuneus	30675	-13	-71	30	2.92

Supplementary Table 9. Right Striatum volume significant peaks of correlation with cortical thickness in HC.

Brain Areas	**vertex**	**x**	**y**	**z**	**t**
Left Calcarine fissure and surrounding cortex	33295	-11	-92	-19	6.02
Left Precuneus	30561	-1	-64	30	5.86
Left Superior frontal gyrus, medial orbital	16899	-5	56	-14	5.85
Left Lingual gyrus	39387	-12	-87	-20	5.83
Left Median cingulate and paracingulate gyri	30717	-5	-41	48	5.53
Left Inferior frontal gyrus, triangular part	19949	-43	30	21	5.45
Left Inferior frontal gyrus, opercular part	20044	-48	13	24	5.33
Left Middle frontal gyrus	19179	-40	32	19	5.29
Left Gyrus Rectus	4261	-4	56	-15	5.2
Left Middle occipital gyrus	8596	-46	-70	16	5.15
Left Fusiform gyrus	9424	-37	-57	-20	4.67
Left Inferior occipital gyrus	35622	-45	-66	-5	4.66
Left Supplementary motor area	7023	-6	5	46	4.63
Left Posterior cingulate gyrus	30229	-3	-53	19	4.61

Left Precentral gyrus	20657	-44	9	24	4.49
Left Superior frontal gyrus, dorsolateral	26093	-21	27	59	4.28
Left Superior occipital gyrus	32420	-29	-86	29	4.28
Left Superior frontal gyrus, medial	444	-8	53	43	4.27
Left Middle temporal gyrus	34872	-51	-54	15	4.21
Left Superior parietal gyrus	25145	-31	-55	65	4.2
Left Insula	10525	-39	-17	5	4.17
Left Cuneus	9614	-18	-53	1	4.16
Left Postcentral gyrus	25000	-27	-37	62	4.1
Left Inferior temporal gyrus	35914	-61	-56	-8	4.1
Left Rolandic operculum	21690	-39	-12	17	3.98
Left Heschl gyrus	2642	-39	-19	4	3.96
Left Angular gyrus	5941	-45	-48	47	3.91
Left Superior temporal gyrus	2616	-40	-18	0	3.9
Left Inferior parietal, but supramarginal and angular gyri	23644	-45	-47	46	3.87
Left Middle frontal gyrus orbital part	4774	-37	58	3	3.85
Left Olfactory Cortex	16045	-3	16	-14	3.81
Left Supramarginal gyrus	22367	-51	-38	24	3.81
Left Anterior cingulate and paracingulate gyri	15430	-5	25	-14	3.67

Left Paracentral lobule	30989	-13	-44	64	3.27
Left Supeiror frontal gyrus, orbital part	15200	-11	37	-23	2.99
Left Temporal pole: superior temporal gyrus	3307	-44	18	-19	2.73
Left Inferior frontal gyrus, orbital part	4808	-42	46	-2	2.68
Left Parahippocampal gyrus	3614	-27	0	-23	2.61
Left Temporal pole: middle temporal gyrus	3340	-48	12	-30	2.47
Right Median cingulate and paracingulate gyri	29254	-11	-15	44	6.22
Right Supplementary motor area	27989	-8	2	46	5.85
Right Superior temporal gyrus	10884	-59	-8	-7	5.74
Right Posterior cingulate gyrus	7574	-4	-48	35	5.73
Right Middle frontal gyrus	1166	-33	44	28	5.65
Right Middle occipital gyrus	34407	-43	-83	13	5.56
Right Inferior frontal gyrus, triangular part	19399	-54	32	9	5.55
Right Paracentral lobule	29429	-8	-25	46	5.49
Right Anterior cingulate and paracingulate gyri	28019	-4	48	27	5.35
Right Precuneus	40664	-6	-48	2	5.34
Right Superior frontal gyrus, medial	27624	-4	50	28	5.26
Right Supramarginal gyrus	22224	-45	-29	16	5.25
Right Olfactory Cortex	16042	-3	15	-15	5.16

Right Supeiror frontal gyrus, orbital part	3507	-25	33	-22	5.13
Right Middle temporal gyrus	10914	-55	-5	-14	5.05
Right Lingual gyrus	39373	-14	-83	-18	4.91
Right Superior occipital gyrus	34019	-26	-84	18	4.78
Right Insula	12731	-36	23	-2	4.77
Right Rolandic operculum	21834	-43	-24	19	4.73
Right Heschl gyrus	11075	-44	-30	11	4.58
Right Superior frontal gyrus, medial orbital	17547	-7	72	-6	4.55
Right Superior frontal gyrus, dorsolateral	27271	-25	51	37	4.44
Right Inferior occipital gyrus	8436	-39	-90	-4	4.44
Right Fusiform gyrus	9422	-35	-54	-19	4.41
Right Parahippocampal gyrus	915	-27	2	-23	4.36
Right Inferior frontal gyrus, opercular part	5161	-46	14	28	4.21
Right Postcentral gyrus	22201	-48	-23	19	4.18
Right Inferior frontal gyrus, orbital part	19170	-50	35	-7	4.16
Right Inferior temporal gyrus	36752	-44	-26	-22	4.14
Right Temporal pole: superior temporal gyrus	14367	-27	2	-24	4.08
Right Cuneus	38474	-16	-60	10	3.98
Right Middle frontal gyrus orbital part	18538	-23	51	-14	3.94

Right Inferior parietal, but supramarginal and angular gyri	5892	-43	-45	43	3.89
Right Calcarine fissure and surrounding cortex	9864	-11	-88	-20	3.82
Right Angular gyrus	5611	-62	-51	33	3.81
Right Superior parietal gyrus	25245	-27	-57	66	3.79
Right Precentral gyrus	20433	-40	4	38	3.65
Right Gyrus Rectus	15270	-11	27	-23	3.46
Right Temporal pole: middle temporal gyrus	3374	-53	9	-39	3.45

Supplementary Table 10. Right Striatum volume significant peaks of correlation with cortical thickness in AD.

Brain Areas	**vertex**	**x**	**y**	**z**	**t**
Left Olfactory Cortex	16045	-3	16	-14	4.72
Left Temporal pole: superior temporal gyrus	13190	-48	18	-33	4.69
Left Temporal pole: middle temporal gyrus	13483	-47	18	-35	4.63
Left Middle temporal gyrus	13321	-51	14	-32	4.58
Left Superior temporal gyrus	3199	-44	0	-14	4.57
Left Inferior occipital gyrus	33470	-36	-88	-17	4.42
Left Anterior cingulate and paracingulate gyri	16057	-2	17	-11	4.25
Left Precentral gyrus	20860	-55	-4	30	4.2
Left Gyrus Rectus	15776	-11	19	-23	4.08

Left Postcentral gyrus	5245	-54	-5	28	4.03
Left Superior frontal gyrus, medial orbital	1018	-3	24	-16	3.81
Left Inferior frontal gyrus, triangular part	11946	-31	26	8	3.69
Left Supramarginal gyrus	21935	-62	-35	34	3.66
Left Fusiform gyrus	35425	-37	-77	-15	3.52
Left Insula	3193	-42	-3	-12	3.51
Left Middle occipital gyrus	33487	-37	-89	-10	3.48
Left Rolandic operculum	5063	-54	9	-1	3.45
Left Inferior frontal gyrus, opercular part	20117	-51	10	-2	3.35
Left Inferior parietal, but supramarginal and angular gyri	21485	-62	-34	41	3.33
Right Anterior cingulate and paracingulate gyri	16540	-1	38	12	5.24
Right Supramarginal gyrus	5387	-52	-29	43	4.55
Right Superior temporal gyrus	12707	-44	1	-14	4.45
Right Temporal pole: superior temporal gyrus	13034	-44	4	-16	4.38
Right Inferior parietal, but supramarginal and angular gyri	22732	-47	-30	42	4.3
Right Temporal pole: middle temporal gyrus	3429	-42	9	-41	4.28
Right Inferior temporal gyrus	13600	-41	8	-44	4.19
Right Middle temporal gyrus	13438	-55	4	-35	4.14
Right Inferior frontal gyrus, triangular part	19502	-40	20	7	3.96

Right Postcentral gyrus	21313	-51	-26	38	3.96
Right Rolandic operculum	21847	-39	-21	17	3.93
Right Inferior frontal gyrus, opercular part	19526	-42	20	7	3.89
Right Superior frontal gyrus, dorsolateral	17856	-18	58	26	3.78
Right Heschl gyrus	10628	-36	-28	18	3.68
Right Olfactory Cortex	15994	-2	16	-16	3.64
Right Insula	10569	-36	-23	16	3.61
Right Middle occipital gyrus	8639	-37	-88	16	3.59
Right Superior parietal gyrus	24343	-38	-39	58	3.54
Right Superior frontal gyrus, medial orbital	4031	-3	22	-16	3.48
Right Precuneus	7939	-11	-76	49	3.46
Right Superior frontal gyrus, medial	4460	-16	59	26	3.42
Right Precentral gyrus	20661	-46	9	25	3.38
Right Inferior frontal gyrus, orbital part	13923	-24	27	-19	3.26
Right Lingual gyrus	39399	-20	-79	-17	3.24
Right Superior frontal gyrus, orbital part	13927	-24	28	-19	3.23
Right Fusiform gyrus	13717	-28	2	-43	3.21
Right Middle frontal gyrus	26755	-23	4	56	3.15

Supplementary Table 11. Left nucleus accumbens volume significant peaks of correlation with cortical thickness for ALL participants.

Brain Areas	**vertex**	**x**	**y**	**z**	**t**
Left Calcarine fissure and surrounding cortex	33204	-10	-92	-19	5.92
Left Lingual gyrus	39386	-10	-86	-19	5.25
Left Olfactory Cortex	16046	-3	15	-13	5.09
Left Anterior cingulate and paracingulate gyri	16057	-2	17	-11	4.84
Left Cuneus	38621	-15	-64	7	4.64
Left Gyrus Rectus	16944	-2	60	-18	4.6
Left Superior frontal gyrus, medial orbital	16951	-2	60	-14	4.39
Left Superior parietal gyrus	6284	-27	-37	61	4.17
Left Superior temporal gyrus	22384	-45	-34	17	4.15
Left Postcentral gyrus	24999	-28	-37	62	4.12
Left Middle frontal gyrus	25975	-23	26	41	4.08
Left Superior frontal gyrus, dorsolateral	25993	-22	27	41	3.96
Left Inferior frontal gyrus, opercular part	4909	-38	17	5	3.95
Left Middle temporal gyrus	13324	-52	10	-28	3.89
Left Rolandic operculum	328	-48	5	1	3.88
Left Inferior frontal gyrus, triangular part	19219	-50	33	13	3.87
Left Heschl gyrus	11076	-45	-29	11	3.82

Left Precuneus	38525	-17	-60	15	3.8
Left Superior frontal gyrus, medial	28222	-6	32	38	3.79
Left Middle occipital gyrus	33446	-33	-93	-10	3.77
Left Temporal pole: superior temporal gyrus	3342	-53	7	-23	3.75
Left Inferior occipital gyrus	33441	-32	-94	-12	3.74
Left Supramarginal gyrus	5586	-45	-34	18	3.73
Left Parahippocampal gyrus	38021	-29	-35	-6	3.66
Left Supplementary motor area	28296	-7	21	47	3.64
Left Supeiror frontal gyrus, orbital part	17132	-8	65	-20	3.63
Left Inferior temporal gyrus	35934	-60	-50	-13	3.6
Left Angular gyrus	23298	-48	-54	27	3.52
Left Insula	12064	-32	18	11	3.51
Left Temporal pole: middle temporal gyrus	3340	-48	12	-30	3.47
Left Precentral gyrus	26763	-23	-4	54	3.45
Left Median cingulate and paracingulate gyri	7483	-5	-18	44	3.38
Left Inferior parietal, but supramarginal and angular gyri	6032	-27	-65	35	3.07
Left Fusiform gyrus	9175	-42	-15	-26	3.05
Left Middle frontal gyrus orbital part	18981	-33	58	3	2.99
Left Superior occipital gyrus	24141	-27	-66	32	2.95

Left Inferior frontal gyrus, orbital part	18643	-39	52	-13	2.94
Left Paracentral lobule	30994	-12	-44	65	2.56
Left Posterior cingulate gyrus	40909	-2	-52	16	2.48
Right Superior temporal gyrus	11384	-65	-15	-3	5.75
Right Median cingulate and paracingulate gyri	29746	-11	-20	41	5.45
Right Middle temporal gyrus	9116	-52	-46	9	5.4
Right Temporal pole: middle temporal gyrus	853	-52	13	-40	5.38
Right Lingual gyrus	39369	-15	-82	-18	5.27
Right Supramarginal gyrus	22416	-54	-37	20	5.08
Right Middle frontal gyrus	19591	-31	38	30	5.04
Right Inferior frontal gyrus, triangular part	19366	-38	26	5	5.02
Right Heschl gyrus	11311	-57	-14	7	4.91
Right Olfactory Cortex	15923	-7	7	-18	4.88
Right Inferior temporal gyrus	13591	-44	6	-42	4.84
Right Precuneus	31620	-10	-76	53	4.73
Right Insula	10537	-39	-19	5	4.66
Right Superior parietal gyrus	31652	-12	-73	51	4.64
Right Superior frontal gyrus, dorsolateral	17921	-23	58	19	4.57
Right Anterior cingulate and paracingulate gyri	16045	-3	16	-14	4.57

Right Angular gyrus	24041	-28	-67	33	4.52
Right Inferior parietal, but supramarginal and angular gyri	390	-27	-65	33	4.45
Right Calcarine fissure and surrounding cortex	39283	-9	-83	-15	4.42
Right Cuneus	31925	-16	-65	19	4.41
Right Middle occipital gyrus	24060	-28	-67	32	4.41
Right Postcentral gyrus	6134	-41	-34	58	4.31
Right Posterior cingulate gyrus	29964	0	-33	33	4.17
Right Temporal pole: superior temporal gyrus	13495	-46	21	-35	4.1
Right Superior occipital gyrus	34019	-26	-84	18	4.02
Right Inferior frontal gyrus, opercular part	4908	-41	20	7	3.95
Right Superior frontal gyrus, medial	4440	-4	52	25	3.94
Right Fusiform gyrus	37897	-25	-76	-13	3.85
Right Supplementary motor area	7386	-7	-21	45	3.81
Right Paracentral lobule	29424	-8	-24	46	3.79
Right Precentral gyrus	21025	-39	-18	43	3.77
Right Rolandic operculum	5489	-41	-24	19	3.76
Right Inferior frontal gyrus, orbital part	19169	-51	38	-7	3.62
Right Gyrus Rectus	15273	-12	25	-22	3.56
Right Supeiror frontal gyrus, orbital part	15242	-12	26	-24	3.49

Right Superior frontal gyrus, medial orbital	76	-6	70	-11	3.35
Right Inferior occipital gyrus	33607	-35	-91	-7	3.2
Right Middle frontal gyrus orbital part	18445	-28	55	-1	3.11
Right Parahippocampal gyrus	915	-27	2	-23	2.79

Supplementary Table 12. Left nucleus accumbens volume significant peaks of correlation with cortical thickness for HC.

Brain Areas	**vertex**	**x**	**y**	**z**	**t**
Left Calcarine fissure and surrounding cortex	33297	-12	-94	-18	6.27
Left Superior frontal gyrus, medial orbital	4262	-4	58	-14	5.53
Left Gyrus Rectus	16932	-3	58	-15	5.33
Left Lingual gyrus	39387	-12	-87	-20	4.64
Left Inferior frontal gyrus, triangular part	19189	-44	34	16	4.34
Left Middle frontal gyrus	20442	-48	24	33	4.07
Left Middle occipital gyrus	34523	-45	-75	28	4.03
Left Superior frontal gyrus, medial	28109	-4	36	33	4.01
Left Olfactory Cortex	16045	-3	16	-14	3.88
Left Supplementary motor area	7102	-6	22	47	3.87
Left Superior frontal gyrus, dorsolateral	1658	-21	29	59	3.8
Left Postcentral gyrus	24470	-30	-37	61	3.69

Left Median cingulate and paracingulate gyri	29550	-5	-40	48	3.67
Left Supeiror frontal gyrus, orbital part	17132	-8	65	-20	3.65
Left Precuneus	9613	-16	-51	0	3.62
Left Superior parietal gyrus	104	-29	-37	60	3.6
Left Middle temporal gyrus	8695	-43	-66	21	3.53
Left Cuneus	38543	-17	-62	16	3.41
Left Angular gyrus	34660	-43	-67	23	3.4
Left Superior temporal gyrus	13304	-53	4	-20	3.23
Left Anterior cingulate and paracingulate gyri	16052	-2	19	-12	3.17
Left Inferior frontal gyrus, opercular part	2565	-39	7	7	3.14
Left Inferior occipital gyrus	35577	-48	-72	-10	3.07
Left Rolandic operculum	5438	-48	0	9	3.05
Left Parahippocampal gyrus	38021	-29	-35	-6	2.96
Left Inferior temporal gyrus	9020	-55	-61	-10	2.95
Left Middle frontal gyrus orbital part	18979	-40	55	2	2.94
Right Middle frontal gyrus	18330	-34	42	29	5.77
Right Median cingulate and paracingulate gyri	29455	-12	-23	41	5.71
Right Superior temporal gyrus	11154	-61	-21	12	5.54
Right Inferior frontal gyrus, triangular part	1223	-53	33	10	5.43

Right Heschl gyrus	718	-60	-12	6	5.1
Right Supeiror frontal gyrus, orbital part	4286	-22	51	-15	4.95
Right Olfactory Cortex	16042	-3	15	-15	4.79
Right Anterior cingulate and paracingulate gyri	16046	-3	15	-13	4.74
Right Superior frontal gyrus, dorsolateral	27302	-22	50	38	4.68
Right Paracentral lobule	29429	-8	-25	46	4.59
Right Middle frontal gyrus orbital part	17061	-22	54	-15	4.57
Right Lingual gyrus	39373	-14	-83	-18	4.55
Right Insula	10376	-42	-12	-1	4.54
Right Supramarginal gyrus	5647	-61	-43	27	4.51
Right Supplementary motor area	7386	-7	-21	45	4.43
Right Precuneus	31861	-16	-62	20	4.39
Right Posterior cingulate gyrus	30048	-8	-40	38	4.32
Right Middle temporal gyrus	10776	-55	0	-18	4.3
Right Fusiform gyrus	2371	-31	-58	-19	4.19
Right Middle occipital gyrus	34505	-45	-83	23	4
Right Inferior occipital gyrus	33618	-39	-89	-4	3.99
Right Inferior frontal gyrus, orbital part	18796	-51	40	-12	3.96
Right Superior frontal gyrus, medial orbital	17592	-14	71	-6	3.94

Right Superior parietal gyrus	31649	-11	-74	50	3.9
Right Postcentral gyrus	5525	-60	-16	31	3.88
Right Cuneus	31915	-17	-67	20	3.87
Right Angular gyrus	5897	-33	-53	41	3.84
Right Inferior parietal, but supramarginal and angular gyri	1489	-42	-47	44	3.83
Right Inferior frontal gyrus, opercular part	20609	-39	11	28	3.69
Right Superior occipital gyrus	34045	-31	-77	20	3.63
Right Superior frontal gyrus, medial	17284	-7	55	18	3.61
Right Calcarine fissure and surrounding cortex	9864	-11	-88	-20	3.52
Right Rolandic operculum	10330	-40	-5	15	3.51
Right Temporal pole: middle temporal gyrus	3374	-53	9	-39	3.49
Right Precentral gyrus	5175	-38	9	29	3.48
Right Parahippocampal gyrus	14368	-27	1	-23	3.17
Right Inferior temporal gyrus	36718	-43	-23	-22	3.15
Right Gyrus Rectus	15034	-6	52	-26	3.08
Right Temporal pole: superior temporal gyrus	14405	-27	3	-23	3.02

Supplementary Table 13. Right precommisural putamen volume significant peaks of correlation with cortical thickness for ALL participants.

Brain Areas	**vertex**	**x**	**y**	**z**	**t**

Left Precuneus	31341	-3	-69	45	4.94
Left Middle frontal gyrus	18965	-32	56	7	4.74
Left Lingual gyrus	2475	-13	-86	-19	4.43
Left Insula	2639	-40	-16	4	4.36
Left Middle frontal gyrus orbital part	18981	-33	58	3	4.35
Left Calcarine fissure and surrounding cortex	39420	-13	-89	-20	4.34
Left Middle temporal gyrus	13331	-53	12	-30	4.25
Left Inferior occipital gyrus	33458	-32	-94	-14	4.21
Left Temporal pole: superior temporal gyrus	13188	-49	16	-30	4.2
Left Temporal pole: middle temporal gyrus	13285	-48	13	-30	4.09
Left Inferior temporal gyrus	35837	-50	-50	-20	4.08
Left Heschl gyrus	2642	-39	-19	4	3.98
Left Superior temporal gyrus	22418	-53	-36	19	3.9
Left Olfactory Cortex	15928	-5	9	-18	3.88
Left Precentral gyrus	20887	-53	-5	30	3.78
Left Superior frontal gyrus, dorsolateral	6554	-23	24	57	3.73
Left Fusiform gyrus	37217	-46	-42	-21	3.73
Left Inferior frontal gyrus, triangular part	19050	-40	45	7	3.7
Left Median cingulate and paracingulate gyri	29797	-1	-22	42	3.7

Left Superior frontal gyrus, medial	27542	-7	55	42	3.61
Left Superior frontal gyrus, medial orbital	4262	-4	58	-14	3.61
Left Gyrus Rectus	15220	-9	36	-24	3.61
Left Inferior frontal gyrus, opercular part	20608	-40	12	28	3.57
Left Supeiror frontal gyrus, orbital part	18442	-27	54	1	3.55
Left Middle occipital gyrus	33446	-33	-93	-10	3.53
Left Supramarginal gyrus	22355	-53	-39	25	3.51
Left Postcentral gyrus	20865	-53	-6	29	3.46
Left Posterior cingulate gyrus	40909	-2	-52	16	3.41
Left Superior parietal gyrus	31636	-11	-74	58	3.38
Left Anterior cingulate and paracingulate gyri	16057	-2	17	-11	3.37
Left Cuneus	32792	-3	-86	28	3.34
Left Rolandic operculum	21802	-46	-23	19	3.31
Left Inferior parietal, but supramarginal and angular gyri	23463	-33	-55	42	3.11
Left Superior occipital gyrus	33892	-28	-84	23	3.07
Left Supplementary motor area	6665	-16	16	66	2.99
Left Angular gyrus	23487	-35	-57	43	2.82
Left Inferior frontal gyrus, orbital part	4808	-42	46	-2	2.6
Right Supramarginal gyrus	22409	-50	-36	20	4.78

Right Median cingulate and paracingulate gyri	7258	-2	3	43	4.76
Right Superior temporal gyrus	22390	-50	-36	19	4.53
Right Lingual gyrus	624	-18	-80	-19	4.51
Right Inferior frontal gyrus, triangular part	19491	-41	22	7	4.43
Right Anterior cingulate and paracingulate gyri	16045	-3	16	-14	4.39
Right Olfactory Cortex	16042	-3	15	-15	4.26
Right Precuneus	30243	-2	-55	18	4.26
Right Rolandic operculum	21834	-43	-24	19	4.23
Right Insula	10531	-38	-19	6	4.19
Right Supplementary motor area	28014	-9	2	44	4
Right Inferior frontal gyrus, opercular part	4904	-38	19	7	3.99
Right Heschl gyrus	10543	-38	-20	5	3.96
Right Posterior cingulate gyrus	30231	-5	-53	22	3.86
Right Temporal pole: middle temporal gyrus	13419	-54	10	-37	3.85
Right Middle temporal gyrus	13409	-56	9	-36	3.82
Right Middle occipital gyrus	2155	-35	-88	22	3.74
Right Inferior temporal gyrus	35845	-49	-53	-17	3.71
Right Superior parietal gyrus	31633	-11	-75	55	3.67
Right Paracentral lobule	29424	-8	-24	46	3.61

Right Temporal pole: superior temporal gyrus	13109	-44	10	-17	3.58
Right Cuneus	31915	-17	-67	20	3.51
Right Postcentral gyrus	22201	-48	-23	19	3.51
Right Superior frontal gyrus, medial	4440	-4	52	25	3.49
Right Fusiform gyrus	36625	-42	-22	-21	3.48
Right Calcarine fissure and surrounding cortex	39428	-16	-89	-19	3.45
Right Middle frontal gyrus	20452	-46	23	29	3.4
Right Inferior frontal gyrus, orbital part	19161	-52	37	-5	3.37
Right Superior occipital gyrus	31667	-17	-80	40	3.23
Right Superior frontal gyrus, dorsolateral	18009	-25	52	34	3.13
Right Superior frontal gyrus, medial orbital	15996	-1	18	-17	3.11
Right Inferior occipital gyrus	35407	-48	-63	-10	3.03
Right Inferior parietal, but supramarginal and angular gyri	23511	-45	-45	46	3.02
Right Supeiror frontal gyrus, orbital part	13938	-25	31	-18	2.86
Right Parahippocampal gyrus	14247	-24	2	-26	2.83
Right Angular gyrus	24035	-27	-66	34	2.82
Right Precentral gyrus	21025	-39	-18	43	2.75
Right Middle frontal gyrus orbital part	18981	-33	58	3	2.63

Supplementary Table 14. Right precommisural putamen volume significant peaks of correlation with cortical thickness for HC.

Brain Areas	**vertex**	**x**	**y**	**z**	**t**
Left Calcarine fissure and surrounding cortex	33299	-13	-92	-18	5.84
Left Median cingulate and paracingulate gyri	29831	-8	-21	43	5.21
Left Lingual gyrus	39421	-14	-88	-20	5.1
Left Middle frontal gyrus	19041	-40	53	8	4.61
Left Middle occipital gyrus	34574	-44	-69	18	4.41
Left Superior frontal gyrus, medial orbital	4262	-4	58	-14	4.33
Left Inferior frontal gyrus, triangular part	19188	-45	34	16	4.28
Left Precuneus	31342	-4	-67	44	4.21
Left Gyrus Rectus	16932	-3	58	-15	4.02
Left Inferior occipital gyrus	576	-59	-60	-9	3.92
Left Insula	2639	-40	-16	4	3.88
Left Superior frontal gyrus, medial	27542	-7	55	42	3.82
Left Posterior cingulate gyrus	30166	-3	-37	37	3.81
Left Inferior temporal gyrus	35940	-59	-59	-9	3.81
Left Superior occipital gyrus	8131	-28	-85	31	3.78
Left Middle temporal gyrus	35910	-61	-54	-7	3.75
Left Superior frontal gyrus, dorsolateral	26560	-21	19	61	3.61

Left Heschl gyrus	2642	-39	-19	4	3.53
Left Inferior frontal gyrus, opercular part	20149	-50	13	22	3.46
Left Middle frontal gyrus orbital part	19079	-42	52	1	3.32
Left Superior temporal gyrus	10435	-41	-18	-1	3.28
Left Supplementary motor area	28231	-3	24	37	3.21
Left Fusiform gyrus	153	-34	-51	-20	3.15
Left Cuneus	32804	-2	-89	28	3.08
Left Rolandic operculum	10626	-35	-27	18	3.01
Left Angular gyrus	23401	-49	-68	33	3.01
Left Supramarginal gyrus	21863	-37	-29	19	2.98
Left Precentral gyrus	26769	-24	-3	54	2.88
Left Anterior cingulate and paracingulate gyri	16778	-9	43	15	2.88
Left Supeiror frontal gyrus, orbital part	17100	-14	63	-11	2.79
Left Postcentral gyrus	22201	-48	-23	19	2.78
Right Median cingulate and paracingulate gyri	28922	-1	1	43	5.39
Right Inferior frontal gyrus, triangular part	19223	-52	33	11	4.45
Right Precuneus	30243	-2	-55	18	4.4
Right Posterior cingulate gyrus	30225	-4	-53	22	4.2
Right Superior frontal gyrus, medial orbital	4394	-3	68	-8	4.04

Right Insula	12731	-36	23	-2	4.04
Right Middle frontal gyrus	20386	-41	16	35	3.99
Right Supplementary motor area	28008	-8	5	42	3.98
Right Middle occipital gyrus	34407	-43	-83	13	3.93
Right Superior frontal gyrus, medial	4415	-4	69	-5	3.88
Right Supramarginal gyrus	22221	-49	-32	18	3.86
Right Inferior temporal gyrus	35811	-59	-52	-24	3.81
Right Anterior cingulate and paracingulate gyri	16045	-3	16	-14	3.75
Right Olfactory Cortex	16042	-3	15	-15	3.74
Right Middle temporal gyrus	34636	-50	-62	10	3.72
Right Heschl gyrus	10543	-38	-20	5	3.68
Right Rolandic operculum	21836	-40	-25	19	3.65
Right Superior temporal gyrus	10906	-57	-3	-13	3.58
Right Supeiror frontal gyrus, orbital part	17593	-15	70	-8	3.53
Right Cuneus	31552	-16	-80	38	3.49
Right Superior frontal gyrus, dorsolateral	17582	-14	71	-2	3.24
Right Angular gyrus	5611	-62	-51	33	3.17
Right Paracentral lobule	7387	-7	-24	47	3.17
Right Fusiform gyrus	36625	-42	-22	-21	3.14

Right Inferior occipital gyrus	8436	-39	-90	-4	3.12
Right Inferior frontal gyrus, opercular part	19519	-44	20	8	3.1
Right Superior occipital gyrus	31667	-17	-80	40	3.08
Right Middle frontal gyrus orbital part	18661	-29	57	-15	3.05
Right Postcentral gyrus	22201	-48	-23	19	3.02
Right Parahippocampal gyrus	915	-27	2	-23	2.97
Right Lingual gyrus	39373	-14	-83	-18	2.96
Right Temporal pole: superior temporal gyrus	3623	-28	4	-22	2.96
Right Inferior frontal gyrus, orbital part	19170	-50	35	-7	2.93
Right Superior parietal gyrus	24090	-25	-65	34	2.87
Right Inferior parietal, but supramarginal and angular gyri	390	-27	-65	33	2.85

Supplementary Table 15. Right precommisural putamen volume significant peaks of correlation with cortical thickness for AD.

Brain Areas	**vertex**	**x**	**y**	**z**	**t**
Left Superior temporal gyrus	13033	-44	3	-15	4.86
Left Temporal pole: superior temporal gyrus	3278	-44	6	-15	4.53
Left Temporal pole: middle temporal gyrus	13285	-48	13	-30	4.4
Left Middle temporal gyrus	13282	-49	13	-29	4.36
Left Inferior occipital gyrus	33470	-36	-88	-17	4.18

Left Precentral gyrus	20887	-53	-5	30	3.94
Left Postcentral gyrus	5245	-54	-5	28	3.76